

## Lithosphere

### Tectonic development of the northeastern Tibetan Plateau as constrained by high-resolution deep seismic-reflection data

Rui Gao, Haiyan Wang, An Yin, Shuwen Dong, Zhaoyang Kuang, Andrew V. Zuza, Wenhui Li and Xiaosong Xiong

*Lithosphere* 2013;5;555-574  
doi: 10.1130/L293.1

---

**Email alerting services** click [www.gsapubs.org/cgi/alerts](http://www.gsapubs.org/cgi/alerts) to receive free e-mail alerts when new articles cite this article

**Subscribe** click [www.gsapubs.org/subscriptions/](http://www.gsapubs.org/subscriptions/) to subscribe to *Lithosphere*

**Permission request** click <http://www.geosociety.org/pubs/copyrt.htm#gsa> to contact GSA

Copyright not claimed on content prepared wholly by U.S. government employees within scope of their employment. Individual scientists are hereby granted permission, without fees or further requests to GSA, to use a single figure, a single table, and/or a brief paragraph of text in subsequent works and to make unlimited copies of items in GSA's journals for noncommercial use in classrooms to further education and science. This file may not be posted to any Web site, but authors may post the abstracts only of their articles on their own or their organization's Web site providing the posting includes a reference to the article's full citation. GSA provides this and other forums for the presentation of diverse opinions and positions by scientists worldwide, regardless of their race, citizenship, gender, religion, or political viewpoint. Opinions presented in this publication do not reflect official positions of the Society.

---

#### Notes

# Tectonic development of the northeastern Tibetan Plateau as constrained by high-resolution deep seismic-reflection data

Rui Gao<sup>1,2</sup>, Haiyan Wang<sup>1,2</sup>, An Yin<sup>3,4,\*</sup>, Shuwen Dong<sup>2</sup>, Zhaoyang Kuang<sup>5</sup>, Andrew V. Zuza<sup>3</sup>, Wenhui Li<sup>1,2</sup>, and Xiaosong Xiong<sup>1,2</sup>

<sup>1</sup>LITHOSPHERE RESEARCH CENTRE, INSTITUTE OF GEOLOGY, CHINESE ACADEMY OF GEOLOGICAL SCIENCES, BEIJING 100037, CHINA

<sup>2</sup>KEY LABORATORY OF EARTH PROBE AND GEODYNAMICS, MINISTRY OF LAND AND RESOURCES OF THE PEOPLE'S REPUBLIC OF CHINA, BEIJING 100037, CHINA

<sup>3</sup>DEPARTMENT OF EARTH, PLANETARY, AND SPACE SCIENCES AND INSTITUTE OF PLANETS AND EXOPLANETS, UNIVERSITY OF CALIFORNIA, LOS ANGELES, CALIFORNIA 90095-1567, USA

<sup>4</sup>STRUCTURAL GEOLOGY GROUP, CHINA UNIVERSITY OF GEOSCIENCES (BEIJING), BEIJING 100083, CHINA

<sup>5</sup>GEOPHYSICAL EXPLORATION DIVISION NO. 6, HUADONG PETROLEUM BUREAU, SINOPEC, NANJING 210007, CHINA

## ABSTRACT

A 180-km-long, high-resolution seismic-reflection survey that imaged the entire crust and the uppermost mantle lithosphere was conducted across the northeastern Tibetan Plateau. This work had three aims: (1) to examine whether the left-slip Haiyuan and Tianjing faults defining the margin of NETibet are crustal- or lithospheric-scale structures, (2) to determine whether seismic fabrics are consistent with middle- and/or lower-crustal channel flow, and (3) to establish the minimum amount of Cenozoic shortening strain in the region. Analysis of our newly obtained seismic-reflection data suggests that the left-slip Haiyuan and Tianjing faults have multiple strands and cut through the upper and middle crust. The faults likely terminate at a low-angle detachment shear zone in the lower crust, because the flat Moho directly below the projected traces of the faults is continuous. The seismic image displays subvertical zones of highly reflective sequences containing parallel and subhorizontal reflectors that are truncated by seismically transparent regions with irregular shape. The transparent regions in the middle crust are traceable to the seismically transparent lower crust and are interpreted as early Paleozoic plutons emplaced during the construction of the Qilian arc in the region. The presence of the undisturbed subvertical contacts between zones of highly reflective and seismically transparent regions rules out the occurrence of channel flow in the middle crust, as this process would require through-going subhorizontal reflectors bounding the channel above and below. The lack of continuous reflectors longer than a few kilometers in the lower crust makes a laminar mode of channel flow unfavorable, but lateral lower-crustal flow could have occurred via small-scale ductile deformation involving folding (less than a few kilometers in wavelength and amplitude). Integrating surface geology and the seismic data, we find that the upper crust along a segment of the seismic surveying line experienced up to 46% crustal shortening postdating the Cretaceous and is thus interpreted as entirely accumulated in the Cenozoic. If the estimated shortening strain is representative across northeastern Tibet, its magnitude is sufficient to explain the current elevation of the region without an appeal for additional contributing factors such as channel flow and/or a thermal event in the upper mantle.

LITHOSPHERE, v. 5; no. 6; p. 555–574; GSA Data Repository Item 2013356 | Published online 15 November 2013

doi: 10.1130/L293.1

## INTRODUCTION

The formation and modification of the current morphology of the Tibetan Plateau have been attributed to: (1) vertically coherent shortening of the entire lithosphere (e.g., England and Houseman, 1986; Dewey et al., 1988), (2) decoupling of crustal and mantle shortening along subhorizontal décollements in the middle and lower crust (e.g., Burchfiel et al., 1989; C.S. Wang et al., 2011), (3) mid- and lower-crustal channel flow (e.g., Zhao and Morgan, 1987; Bird, 1991; Royden et al., 1997; Clark and Royden, 2000), (4) convective removal of Tibetan mantle lithosphere leading to plateau uplift (e.g., England and Houseman, 1989; Harrison et al., 1992; Molnar et al., 1993), and (5) continental

subduction with or without coupling of strike-slip faulting (e.g., Wang et al., 2001; Tapponnier et al., 2001). Each of these models predicts specific crustal structures and strain distribution within the plateau interior and along the plateau margins that can be tested by the analysis of high-resolution seismic-reflection studies (e.g., Hubbard and Shaw, 2009; C.S. Wang et al., 2011). For example, the midcrustal décollement model of Burchfiel et al. (1989) requires major thrusts and strike-slip faults to be restricted to the upper crust. Conversely, neither the channel-flow model of Clark and Royden (2000) nor the convective-removal model of Molnar et al. (1993) requires significant upper-crustal shortening for achieving the current elevation of the Tibetan Plateau. Finally, the vertically coherent deformation model of England and Houseman (1986) requires coupling of crustal and upper-

mantle deformation and thus a lack of subhorizontal décollements.

In order to test these models, we conducted a high-resolution seismic-reflection investigation across the northeastern Tibetan Plateau (Figs. 1B and 2). Our profile images the entire crust and the uppermost mantle lithosphere (Fig. 3A). The profile crosses a major active strike-slip fault bounding the northeastern plateau edge, the Haiyuan fault (Fig. 2). This structure has been interpreted either as an upper-crustal transpressional transfer fault by Burchfiel et al. (1991) or a strike-slip fault coupled with continental subduction (e.g., Gaudemer et al., 1995). The main goal of this study is to establish the first-order lithospheric structures imaged in the seismic-reflection profile and to differentiate the two models by examining whether the Haiyuan fault cuts and offsets the Moho. This informa-

\*E-mail: [ayin54@gmail.com](mailto:ayin54@gmail.com).

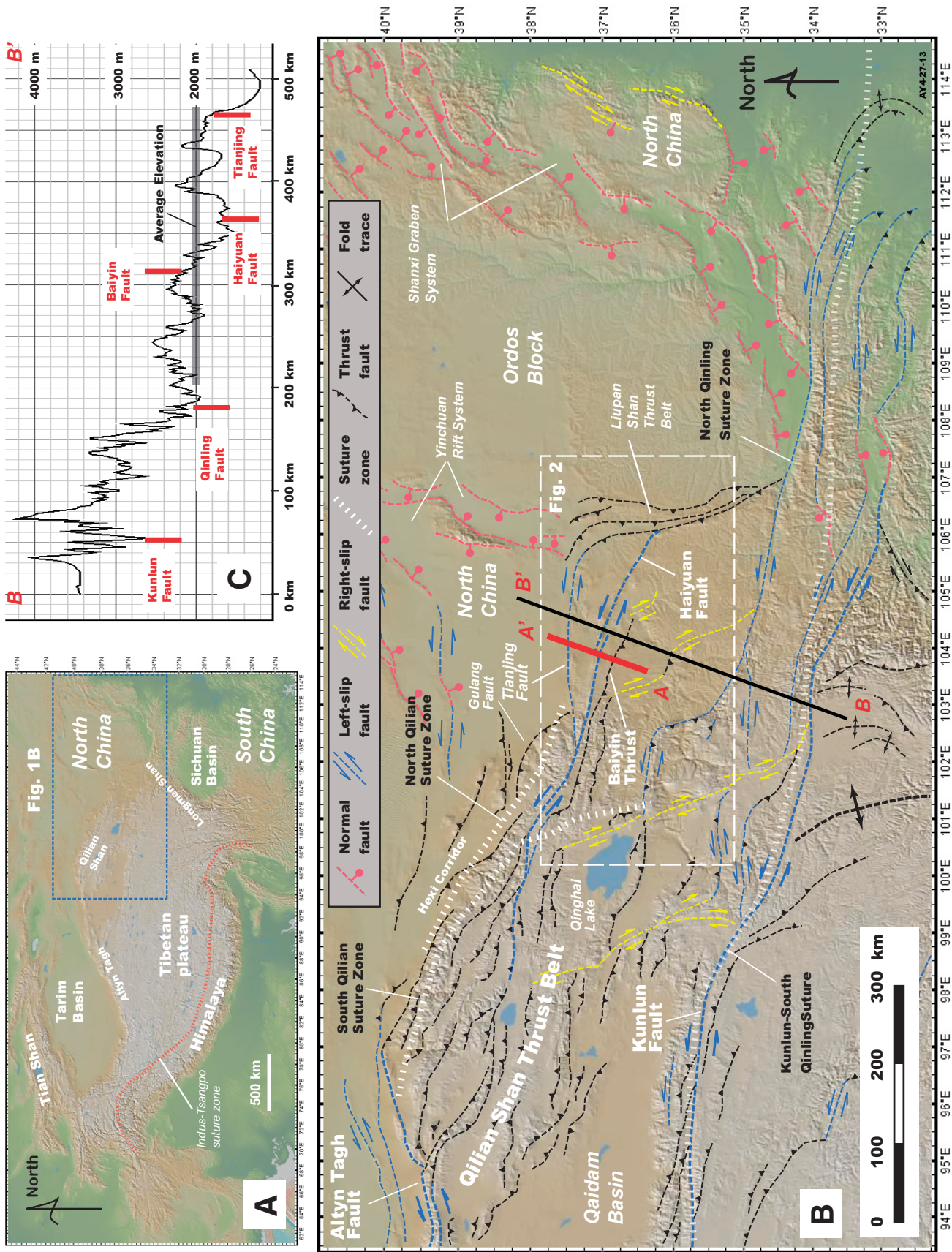
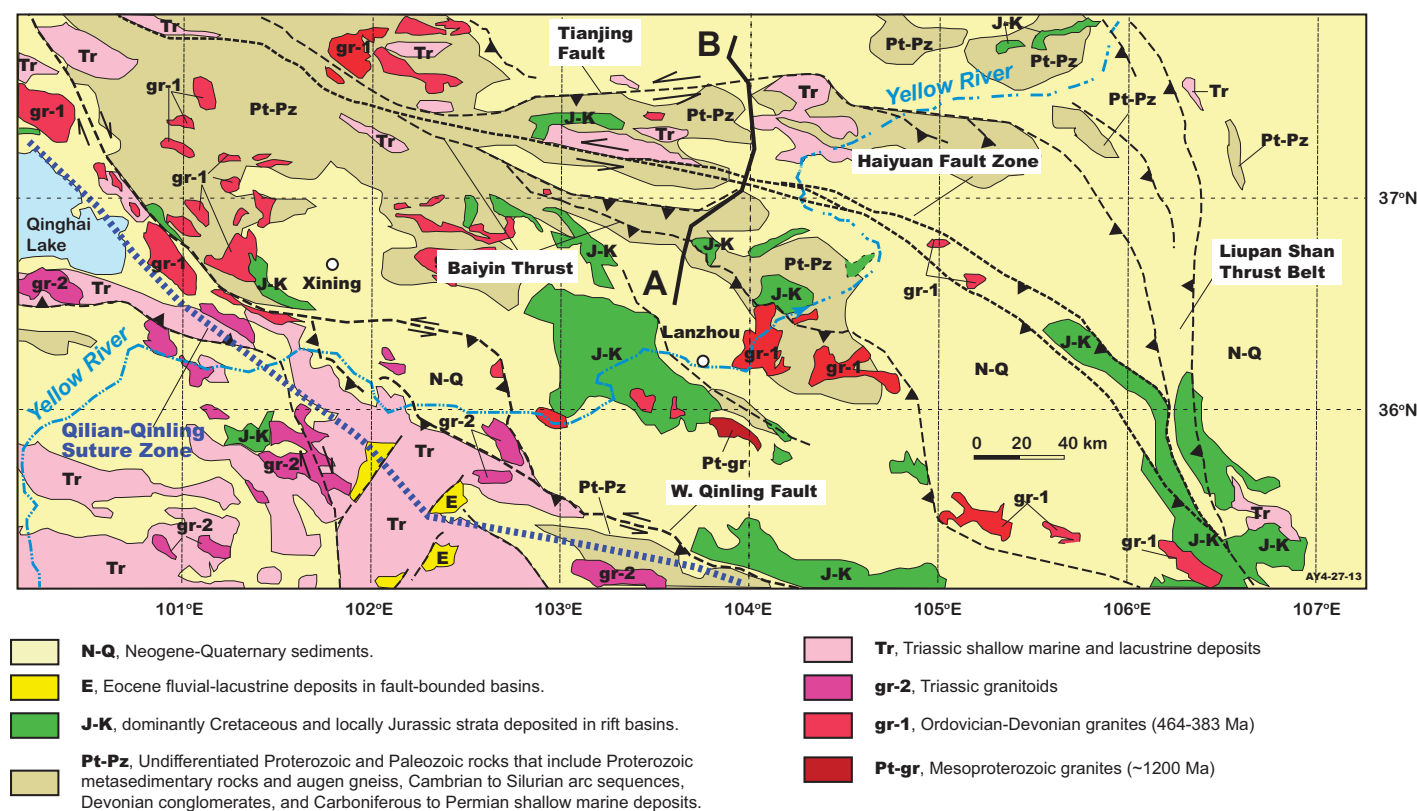


Figure 1. (A) Digital topographic map of the Himalaya, Tibet, and the surrounding region from GeoMapApp.org. Also shown is location of part B and the main regional tectonic features. (B) Map of main Cenozoic faults in the Qilian Shan thrust belt and the location of the seismic-reflection profile shown as profile A-A' obtained from this study. The structures shown in the map follow that of Burchfiel et al. (1991), Gaudemer et al. (1995), and Taylor and Yin (2009). (C) Topographic profile across NE Tibet. Location of the profile is shown as B-B' in B. The digital topographic map and profile were obtained by using GeoMapApp software available at <http://www.geomapp.org/>.



**Figure 2.** Simplified geologic map of NE Tibet from Pan et al. (2004) and the location of seismic profile in thick black line from A to B. See GSA Data Repository (see text footnote 1) for a more detailed geologic map along the seismic survey line.

tion allows us to constrain the deformation history of the region and in particular the mode of Cenozoic deformation leading to the formation of the northeastern Tibetan Plateau.

As seismic-reflection profiles may be interpreted in multiple ways, we take the following approach to ensure the plausibility and testability of our interpreted seismic profiles. Specifically, our interpreted sections must be consistent with: (1) known surface geology, (2) the regional tectonic history, (3) existing geophysical constraints (e.g., vertical distributions of seismic speed and the corresponding rock composition), and (4) the principle of mass conservation, allowing restoration of the interpreted seismic profiles using balanced cross-section methods. The main conclusions reached using this approach are: (1) the Haiyuan fault cuts through the upper and middle crust and terminates at a lower-crust décollement that dips at a moderate dip angle of  $\sim 30^\circ$  to the south, (2) the upper crust locally experienced  $>46\%$  of Cenozoic shortening accommodated by the development of multiple levels of duplex systems, (3) the middle crust and lower crust are dominated by plutonic rocks emplaced during the early Paleozoic development of the Qilian arc, and (4) the Moho is expressed either as a narrow and

concentrated zone of high reflectivity ( $<500$  m) or a wide (4–6 km) and diffuse zone of multiple reflectors serving as transition from the more reflective lower crust above to the nearly nonreflective uppermost mantle below.

## REGIONAL GEOLOGY

### Topography of Northeastern Tibetan Plateau

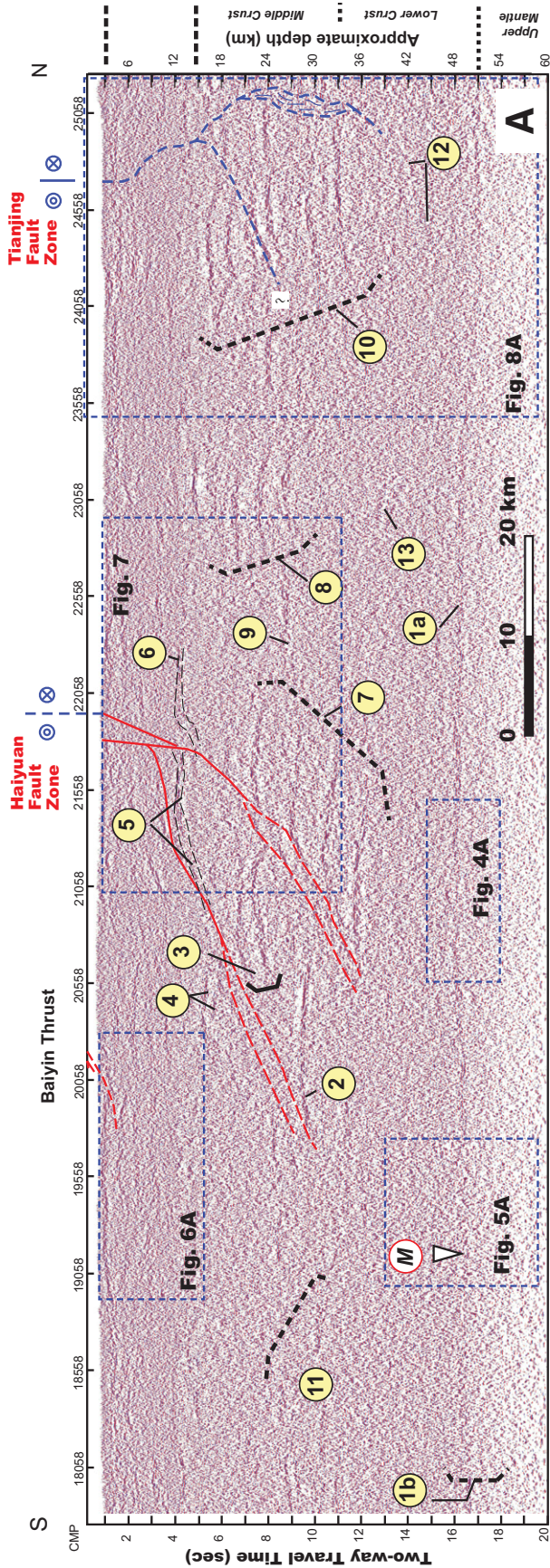
Except its southernmost margin, where the high topography may have been generated by the Mesozoic development of an Andean-type margin (e.g., Murphy et al., 1997), the current topography of the Tibetan Plateau (with an average elevation of  $\sim 5$  km) was mainly created in the Cenozoic during the India-Asia collision (Yin and Harrison, 2000; Tapponnier et al., 2001; Royden et al., 2008). The plateau is bounded by the Himalayan Range south of the Indus-Tsangpo suture and the North China craton in the south and north, respectively (Fig. 1A). In the west and east, the plateau lies against the Tarim and Sichuan Basins with sharply defined margins (Fig. 1A).

In contrast to the sharply defined plateau margins in the north along the Qilian Shan

front, east along the Longmen Shan front, and west along the Altyn Tagh Range, Royden et al. (1997) and Clark and Royden (2000) noted that the northeastern and southwestern corners of the Tibetan Plateau display gradual transition in topography, from the high-altitude (4000–5000 m) plateau interior to the low-altitude plateau foreland (mostly  $<1500$  m) (Fig. 1A). For example, the elevation in northeastern Tibet decreases from  $>4000$  m south of the Kunlun fault to  $<1.5$  km in the foreland of the northeastern Tibetan Plateau over a distance of  $\sim 450$  km (Figs. 1B and 1C). The absence of sharp topographic fronts and the apparent lack of Cenozoic shortening across the gradational plateau margins have been used as evidence for lower-crustal channel flow during Cenozoic development of the Tibetan Plateau (Clark and Royden, 2000; Royden et al., 2008).

### Cenozoic Structures and Deformation History

In the context of Cenozoic fault systems in Tibet (e.g., Taylor and Yin, 2009), the northeastern margin of the Tibetan Plateau is defined by the east-striking, left-slip Haiyuan and Tianjing faults (Burchfiel et al., 1991). The two faults



### Legend

- 1a A strong zone of reflection bounding highly reflective regions above and seismically transparent regions below. Its top surface is interpreted as the Moho.
- 1b An abrupt transition zone separating highly reflective regions above and seismically transparent regions below. This transition zone is interpreted as the Moho.
- M A boundary between the sharply defined Moho surface to the north (right) and a transitional Moho zone to the south (left). It may represent the northern Qilian suture.
- 2 A prominent upward-arching reflector terminating at seismically transparent regions in the south (its left end) and the north (its right end).
- 3 Two subparallel upward-arching reflectors terminating in the south (left) at a seismically transparent region and in the north (right) at the top of reflector sequence (7).
- 4 Two short (3-4 km long) north-dipping reflectors terminating in seismically transparent regions at two ends.
- 5 A zone of strong seismic reflection that is truncated in the north (right) by reflector sequence (6) and terminates in the south (left) at a seismically transparent region.
- 6 A zone of strong reflection with reflectivity decreasing northward (to the right). Its western end terminates in a seismically transparent region.
- 7 A reflector sequence consisting of four major reflective horizons. The lower reflectors are flat whereas upper reflectors warp upward.
- 8 A reflector sequence consisting of four evenly spaced reflective horizons that terminate abruptly in the south. Reflectivity decreases northward.
- 9 A strong reflector between reflector sequences (7) and (8).
- 10 A sequence of eight prominent reflectors spaced irregularly vertically. Lower two reflectors are slightly flatter than antiformal reflectors above.
- 11 A reflector sequence with two prominent reflective horizons terminating to the north (right) at a seismically transparent region.
- 12 A weak, south-dipping reflector in the lower crust. See Fig. 8 for details.
- 13 A localized reflector sequence surrounded by a large seismically transparent region.

Figure 3. (A) Seismic profile obtained from this study that shows the distribution of major reflector sequences labeled sequentially from 1 to 13. The characteristics of each reflector sequence are described in the legend. Also shown are the surface locations of the Baiyin, Haiyuan, and Tianjing faults discussed in the text. Locations of detailed insets of the seismic profile shown in Figures 4-8 are also indicated. (Continued on following page.)

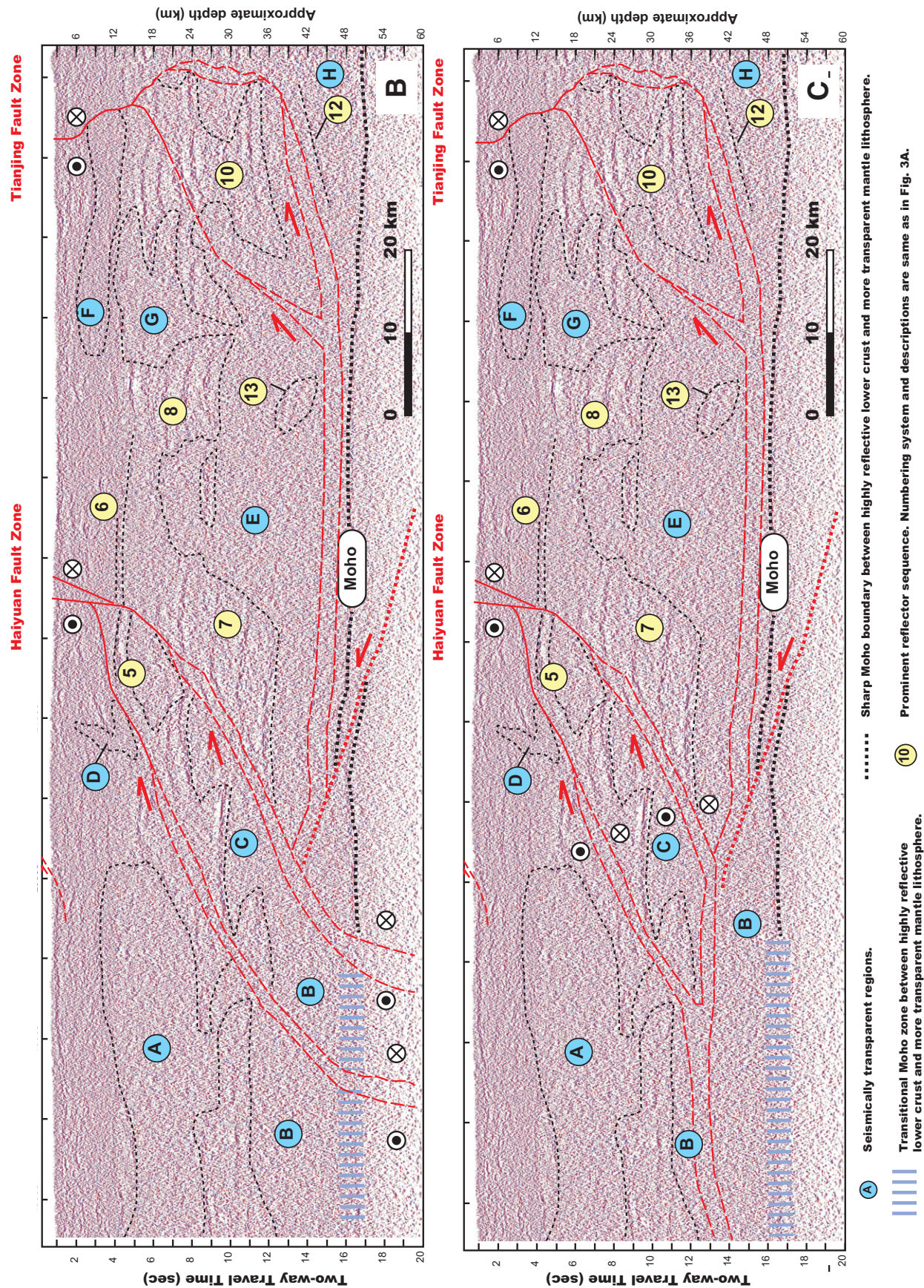


Figure 3 (Continued). (B) The Haiyuan fault is interpreted to cut across the Moho and forms a boundary between the sharp and transitional Moho zone. (C) The Haiyuan fault is interpreted to flatten southward into a subhorizontal shear zone at the base of the middle crust.

link with WNW-striking thrusts of the Qilian Shan to the west and the north-striking thrusts in the Liupan Shan to the east (Fig. 1B). The Haiyuan fault lies within the 1300-km-long and 300-km-wide Cenozoic Qilian Shan thrust belt, which was initiated locally at 50–40 Ma (Jolivet et al., 2001; Dupont-Nivet et al., 2004; Horton et al., 2004; Dai et al., 2006; Yin et al., 2008a, 2008b; Clark et al., 2010; Duvall et al., 2011), followed by widespread development of thrusts and thrust-bounded intermontane basins at 30–20 Ma (Fang et al., 2005; Garzzone et al., 2005; Lease et al., 2007, 2011, 2012a, b; Jin et al., 2010; Craddock et al., 2011; Lin et al., 2011; Zheng et al., 2010; Liu et al., 2011; X. Wang et al., 2011; W.T. Wang et al., 2011; Zhuang et al., 2011; Z. Wang et al., 2012; G. Xiao et al., 2012; H.P. Zhang et al., 2012; Z.Q. Zhang et al., 2013; Lu et al., 2012). Although the Haiyuan fault is the most dominant Cenozoic structure in northeastern Tibet, its total displacement remains debated, with estimates ranging from 20 to 30 km (Burchfiel et al., 1991; P.Z. Zhang et al., 1991) to ~120 km (Gaudemer et al., 1995). Preliminary estimated Quaternary slip rates were as high as 11–19 mm/yr (e.g., Gaudemer et al., 1995; Lasserre et al., 1999, 2002), but recent and more detailed work indicates that the rate is <4 mm/yr (Zheng et al., 2009, 2013; Jolivet et al., 2012).

Cenozoic thrusts in the Qilian Shan involve Precambrian crystalline rocks (e.g., Yin et al., 2007a) that are interpreted to sole into a south-dipping low-angle (i.e., a few degrees) basal thrust (e.g., Burchfiel et al., 1989; Tapponnier et al., 1990; Gaudemer et al., 1995; Meyer et al., 1998) or subhorizontal décollement at a depth of ~15–20 km (Lease et al., 2012b). Specifically, Gaudemer et al. (1995) interpreted that the Haiyuan fault soles into the thrust décollement at a depth of ~20 km. As shown in our study detailed herein, it is impossible to place a through-going décollement at this depth in our study area, and the likely location of a décollement is probably located deeper than 40 km in the lower crust.

Quaternary slip rates on major active thrusts range from 1 to 5 mm/yr (Hetzl et al., 2004; Zheng et al., 2009, 2013; Seong et al., 2011; Yuan et al., 2011; Z.Q. Zhang et al., 2012). The estimated magnitudes of total Cenozoic shortening across the Qilian Shan were mostly obtained from limited available data. Meyer et al. (1998) proposed a total shortening of 150 km across the Qilian Shan based on a balanced cross section constructed by interpreting satellite images. The current lack of field checks for these sections makes this estimate speculative. Van der Woerd et al. (2001) estimated ~9–12 km of shortening across the Danghe Nan Shan thrust, a southernmost thrust in the Qilian Shan thrust

belt. Their estimate was obtained by extrapolating the Holocene slip rates of the fault over a time span of 8 m.y. As the initiation age of the thrust is older than 29 Ma (Yin et al., 2002), the total slip along the fault could be much higher if the Quaternary slip rate can be equated to the time-averaged slip rate of the fault. However, it is possible that the fault slip rate varied with time, and its Quaternary slip rate does not represent its average slip rate. Because of this, it is difficult to extrapolate the Quaternary slip rate for the total slip of the fault.

Gaudemer et al. (1995) constructed a cross section across the Haiyuan fault in the eastern Qilian Shan. Using an area-balance method, they concluded a minimum shortening of 25 km over an original section of 100 km (>25% shortening) accommodated by the Haiyuan and adjacent thrusts. It is important to note that their approach violates the fundamental assumption of the area-balancing method due to the presence of the left-slip Haiyuan fault (i.e., deformation is no longer plane-strain but with out-of-the-plane mass transfer). The lack of well-constrained crustal shortening across the Qilian Shan has prevented quantitative tests of the existing tectonic models described in the introduction.

### Jurassic–Cretaceous Extensional Tectonics and Basin Formation

The Qilian Shan and its neighboring regions (i.e., Hexi corridor to the north, Qaidam Basin to the south, and Altyn Tagh Range to the west) (Fig. 1B) experienced at least two phases of extension in the Jurassic and Cretaceous, respectively (e.g., Chen et al., 2003; Yin et al., 2007a, 2008a, 2008b). The extensional events resulted in the development of east-trending Jurassic and Cretaceous basins bounded by extensional and transtensional faults (e.g., Huo and Tan, 1995; Vincent and Allen, 1999; Chen et al., 2003; Yin et al., 2008a, 2008b). In the eastern Qilian Shan east of longitude 103°E, where our seismic surveying line is located, no Mesozoic extensional faults have been mapped at the surface. However, fining-upward sequences of Cretaceous strata were documented and interpreted as resulting from extensional tectonics (e.g., Vincent and Allen, 1999). It is possible that Cretaceous extensional faults responsible for the formation of the Cretaceous basins are buried below extensive Quaternary deposits in our study area in northeastern Tibet.

### Early Paleozoic Qilian Orogen and its Basement Rocks

The most dominant tectonic event in northern Tibet was the development of the early Paleozoic

Qilian orogeny (e.g., Yin and Harrison, 2000; Gehrels et al., 2003a, 2003b; Yin et al., 2007a; W.J. Xiao et al., 2009; Song et al., 2012, 2013). Current debates on the Qilian orogen are centered on: (1) whether its formation was related to south- and/or north-dipping subduction (e.g., Sobel and Arnaud, 1999; Yin and Harrison, 2000; Gehrels et al., 2003a, 2003b; Yin et al., 2007a; W.J. Xiao et al., 2009; Xu et al., 2010a, 2010b; J. Yang et al., 2009, 2012; Yan et al., 2010; Song et al., 2013), and (2) whether the final closure of the Qilian ocean(s) occurred in the Silurian or Devonian (W.J. Xiao et al., 2009; cf. J. Yang et al., 2012). Regardless of these uncertainties, the existing data suggest that: (1) an open ocean(s) existed in the Qilian Shan region prior to 530 Ma (e.g., Smith, 2006; Tseng et al., 2007; Xia and Song, 2010; Song et al., 2013), (2) oceanic subduction occurred at 477–490 Ma (Su et al., 2004; Zhang et al., 2007), and (3) the Qilian arc was constructed on a thick (at least 5–6 km) Precambrian passive-margin sequence of North China in the western Qilian Shan (west of Qinghai Lake or west of longitude 103°E) and on Precambrian crystalline basement and a thin (<1–2 km) cratonal sequence of North China in the eastern Qilian Shan (east of Qinghai Lake or east of longitude 103°E) (Bian et al., 2001; Xu et al., 2008; Tseng et al., 2009a, 2009b) (Fig. 1B).

In the western Qilian Shan, the Proterozoic passive-margin strata were intruded by 920–930 Ma plutons (Gehrels et al., 2003a, 2003b) and are thrust under an eclogite-bearing metamorphic complex that is interpreted to be part of the early Paleozoic, north-facing Qilian arc (Tseng et al., 2006). The metamorphic complex contains 775–930 Ma orthogneiss (Tseng et al., 2006; Xue et al., 2009; Tung et al., 2007a, 2007b) and paragneiss with older than 880 Ma detrital zircon (Tung et al., 2007a, 2007b). Arc activity at 520–440 Ma in the western Qilian Shan was followed by 435–345 Ma postorogenic magmatism (e.g., Gehrels et al., 2003a; Su et al., 2004; Wu et al., 2004, 2006, 2010; Y.-J. Liu et al., 2006; Quan et al., 2006; He et al., 2007a, b; Tseng et al., 2009a, 2009b; Dang, 2011; Song et al., 2012, 2013; Xia et al., 2012; Xiong et al., 2012).

In the eastern Qilian Shan, Archean to Paleoproterozoic crystalline rocks are intruded by 750–1190 Ma plutons and overlain by a Neoproterozoic cratonal sequence and early Paleozoic arc sequences (Guo et al., 1999; Wan et al., 2001, 2003; H. Wang et al., 2007; Tung et al., 2012) (Fig. 2). Arc magmatism occurred in two discrete phases in the eastern Qilian Shan, at 507–355 Ma related to the formation of the Qilian arc, and at 218–245 Ma during development of the Kunlun arc to the south (Li et al., 2003; Jin et al., 2005; Pei et al., 2005, 2007a, 2007b, 2007c, 2009; Zhang et al., 2006; Chen et

al., 2008a, 2008b; Yong et al., 2008; Dong et al., 2009; Guo et al., 2012; Luo et al., 2012).

The difference in the arc basement clearly controls the style of Cenozoic faults. In the western Qilian Shan, Cenozoic structures are predominantly thin-skinned thrusts that are closely spaced (30–50 km) and laterally continuous over hundreds of kilometers. In contrast, Cenozoic structures in the eastern Qilian Shan are dominated by short-segmented thrusts terminating at strike-slip faults (Figs. 1 and 2).

### Lithospheric Structures of Northern Tibet

Recent geophysical studies have provided first-order constraints on the lithospheric structures of northeastern Tibet. Q. Zhang et al. (2011) used Rayleigh-wave tomography to demonstrate that the mantle lithosphere beneath northeastern Tibet has lower velocities than the mantle lithosphere below North China. H.S. Zhang et al. (2012) estimated the thickness of the Qilian Shan lithosphere to be 145–175 km thick using S-wave receiver functions and SKS splitting measurements. Yue et al. (2012) determined the crustal thickness of the same region to be 65–70 km using the receiver function method. Z.J. Zhang et al. (2011) obtained a crustal thickness of ~62 km under the Songpan–Ganzi terrane and 60–64 km under the Eastern Kunlun Range based a seismic-refraction study. Magnetotelluric (MT) data suggest the possible presence of two imbricated thrust sheets soling into a south-dipping décollement beneath the Qilian Shan (Xiao et al., 2012b).

Although the thicker-than-normal thickness of the crust is well established in northeastern Tibet, the mechanism by which crustal thickening has been achieved has been debated (see a review in Lease et al., 2012b). It has also been debated whether crustal deformation was coupled with mantle deformation during the construction of northeastern Tibet. For example, Moho offset detected by a refraction study across the Kunlun fault has been explained by lower-crustal channel flow (Karplus et al., 2011). In contrast, a high-resolution seismic-reflection study across the same structure indicates ductile thrusting involving both the lower crust and the mantle lithosphere (C.S. Wang et al., 2011). While shear-wave-splitting analysis supports the vertically coherent deformation model across northeast Tibet (J. Li et al., 2011; Y.H. Li et al., 2011), a joint seismic inversion reveals the presence of low-seismic-velocity zones that are interpreted to have accommodated Cenozoic midcrustal channel flow (Y. Yang et al., 2012).

Another major controversy on the formation of the Tibetan Plateau is whether Asian litho-

sphere (i.e., North China craton) has been subducted as a coherent slab underneath northern and central Tibet (e.g., Tapponnier et al., 1990). This is relevant to our study because subduction of continental lithosphere requires Moho offsets, which should be detectable by high-resolution seismic-reflection profiling that images the uppermost mantle lithosphere. Although early receiver-function studies support this notion (Kind et al., 2002; Shi et al., 2004; Kumar et al., 2006; Zhao et al. 2011), recent work by Liang et al. (2012) disputed this suggestion using data from a more densely distributed network of seismic stations in the region. Liang et al. (2012) suggested that the high-velocity bodies below central Tibet represent fragments of the Indian slab rather than a coherent Asian mantle lithosphere from the north.

The main contribution of this study to the current debates on the lithospheric structure of northern Tibet is to provide a detailed seismic image of the whole crust and the uppermost mantle. Integrating the existing seismic-refraction data from the same area (M.J. Liu et al., 2006), we are able to provide new constraints on the likely composition of the seismically imaged structures in the profile as detailed herein.

### SEISMIC-REFLECTION PROFILE

A 180-km-long seismic-reflection survey was conducted across northeast Tibet (see Figs. 1 and 2 for its location). The acquired seismic profile is shown in Figure 3A. Prominent reflectors and reflector sequences in Figure 3A are described in detail in the figure legend and figure caption. Data acquisitions, data processing, and an uninterpreted high-resolution seismic-reflection profile can be found in the GSA Data Repository.<sup>1</sup>

In the display of the seismic profile, we show both the two-way traveltimes and the *approximate* corresponding depths converted from assigning an average seismic velocity of 6 km/s for the entire seismic section. As the velocity of the seismic image varies with depth, the time-depth conversion shown in the seismic profile of Figure 3A distorts the true geometry of the imaged structures. A previous seismic-refraction survey across our study area indicated that the top 5 km of the crust has variable P-wave velocities from 3 km/s to 6 km/s (M.J. Liu et al., 2006). Between 5 km and 50 km at the

base of the crust, the average P-wave velocity increases gradually downward from ~6 km/s to 6.8 km/s with rather minor lateral variations in seismic speed (M.J. Liu et al., 2006). The average P-wave velocity directly beneath the Moho is ~8.0 km/s (M.J. Liu et al., 2006). M.J. Liu et al. (2006) interpreted the middle and lower crust to have an intermediate composition.

The seismic-velocity variation with depth indicates that by using a single average seismic velocity of 6 km/s as in this study, the true structural geometry is either vertically stretched (i.e., in the upper 5 km) or compressed (i.e., in the lower crust and the upper mantle). Because of this effect, the dip angle of an inclined surface would be overestimated in the uppermost crust and underestimated in the lower crust and the upper mantle. This would in turn affect the estimates of horizontal shortening using the line-balancing method. Specifically, the assignment of seismic speed at 6 km/s would stretch the uppermost 5 km of the crust for ~20%–30% and compress the lowermost crust and the upper mantle for ~10%–30% vertically. From a simple geometric relationship, this effect only distorts the length of a gently inclined reflector (<20°–30°) by no more than 5% of its original length. The readers should take this effect into account when reading the results regarding estimating crustal shortening using the line-balancing method. Note that our surface reference datum for all seismic profiles displayed in this study is set to zero at an elevation of 3500 m above sea level (e.g., Fig. 3A). The horizontal spacing of the short vertical ticks at the top of the seismic profiles is 10 km (e.g., Fig. 3A).

Our seismic profile crosses the left-slip Haiyuan and Tianjing faults, Neoproterozoic and Paleozoic volcanic and sedimentary sequences, Devonian to Triassic strata, and Cretaceous basin fills (Figs. 1 and 2). As Archean to Mesoproterozoic metamorphic basement rocks intruded by 750–1190 Ma orthogneiss are present along the edges of Xining and Lanzhou Basins near our seismic-reflection profile (Guo et al., 1999; Wan et al., 2001, 2003; H. Wang et al., 2007; Tung et al., 2012), we project these rocks onto the seismic profile according to their strike, stratigraphic thickness, and structural positions where the information is available.

Early Paleozoic plutons of the Qilian arc are exposed on both sides of our seismic line (e.g., Gao et al., 1999, 2000, 2001; Gehrels et al., 2003a; Song et al., 2012, 2013). Triassic plutons are exposed south of the seismic line (Fig. 2), which were parts of the Kunlun batholith generated by the northward subduction of the Paleotethys ocean(s) (e.g., Yin and Harrison, 2000; Cowgill et al., 2003).

<sup>1</sup>GSA Data Repository Item 2013356, (1) detailed procedures for data acquisition and data processing and (2) the finally obtained seismic image used in the paper without geologic interpretations, is available at [www.geosociety.org/pubs/ft2013.htm](http://www.geosociety.org/pubs/ft2013.htm), or on request from [editing@geosociety.org](mailto:editing@geosociety.org), Documents Secretary, GSA, P.O. Box 9140, Boulder, CO 80301-9140, USA.

## Uppermost Mantle and the Moho Zone

Despite being compressed vertically as a result of a lower assigned P-wave velocity (i.e., 6 km/s rather than actual 8.1 km/s), the upper-

most mantle is characterized by sparsely distributed short reflectors with low reflectivity (Fig. 3A). This gives the upper mantle an appearance of “emptiness” when compared to the seismic fabrics in the lower crust.

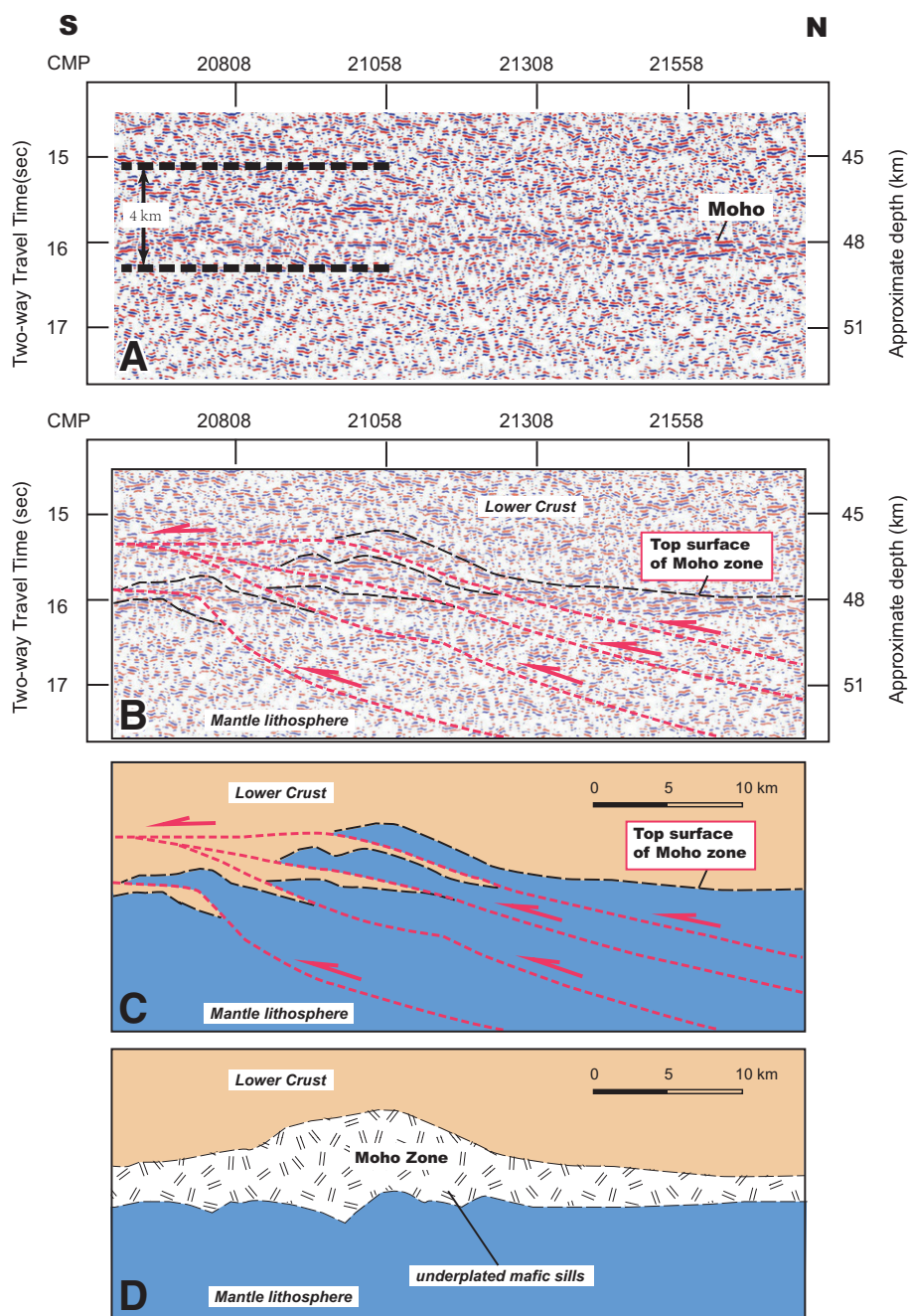


**Figure 4.** (A) A close-up view of a portion of our uninterpreted seismic-reflection profile; see Figure 3A for location. (B) Interpreted seismic-reflection profile from A that shows interpreted thrust shear zones offsetting the Moho defining the upper surface of a high-reflective zone. The zone separates a reflective region above (lower crust) and much less reflective region below (mantle). (C) A sketch of the geology shown in B. In this interpretation, the undulation of the top surface of and discontinuous reflectors within the Moho zone are attributed to movement on several discrete ductile thrust shear zones. (D) Alternative interpretation attributing undulation of the top surface of the Moho zone as a result of local thickening of the highly reflective zone. This could either be a result of deformation or magmatism.

Our interpreted Moho zone directly above the uppermost mantle described earlier herein occurs in two modes: a sharply defined, 300–500 m zone containing long (5–7 km), continuous, and subhorizontal reflectors in the north (i.e., north of point M in Fig. 3A) and a 4–6 km gradient zone in the south (i.e., south of point M in Fig. 3A). The latter is characterized by a downward decrease in seismic reflectivity and the number of seismic reflectors per unit area. Although the highly reflective northern Moho zone has an average thickness of ~300–500 m, its thickness locally reaches to ~8 km (i.e., location of Fig. 4 given in Fig. 3A). As the clusters of long reflectors in the locally thickened northern Moho zone terminate abruptly at their lateral ends, the thickening of the Moho zone could have been induced by north-dipping ductile thrusting (Fig. 4C). Using the upper bounding surface of the Moho zone as a marker and assuming that it was flat before being offset, we obtain 27 km of horizontal shortening that corresponds to a shortening strain of ~36% (Fig. 4C). Alternatively, thickening of the Moho zone could have been induced by magmatic processes resulting from underplating of ductile crustal materials (Fig. 4D). Finally, it is possible that the thickening of the Moho zone was induced by ductile shortening with laterally variable strain.

## Reflectors in the Lower Crust

Directly above the Moho, the density of reflectors in the lower crust increases drastically compared to the upper mantle below the Moho zone. The lower crust is characterized by discontinuous, variably dipping, short in length (<3 km), and locally concave-upward reflectors (Figs. 4 and 5). Longer (>5 km) and straighter reflectors are rare and are only recognized at two locations (i.e., reflectors 12 and 13 in Fig. 3).

Although its lower boundary is marked by the generally flat Moho zone, the upper boundary of the lower-crustal fabrics is poorly defined because the fabrics (i.e., short and disharmonic reflectors) can be traced continuously upward from 45 km to 15 km across parts of the highly reflective middle crust (e.g., regions B, C, E, and H in Figs. 3B and 3C). This observation suggests that the seismically transparent regions in the middle and lower crust may share the same origin (Fig. 3).

## Reflectors in the Middle Crust

Despite the local occurrence of the “lower-crustal” seismic fabrics, the overall seismically defined structures in the middle crust (45–15 km) exhibit reflectors and reflector sequences that are generally subhorizontal (Fig. 3A). In

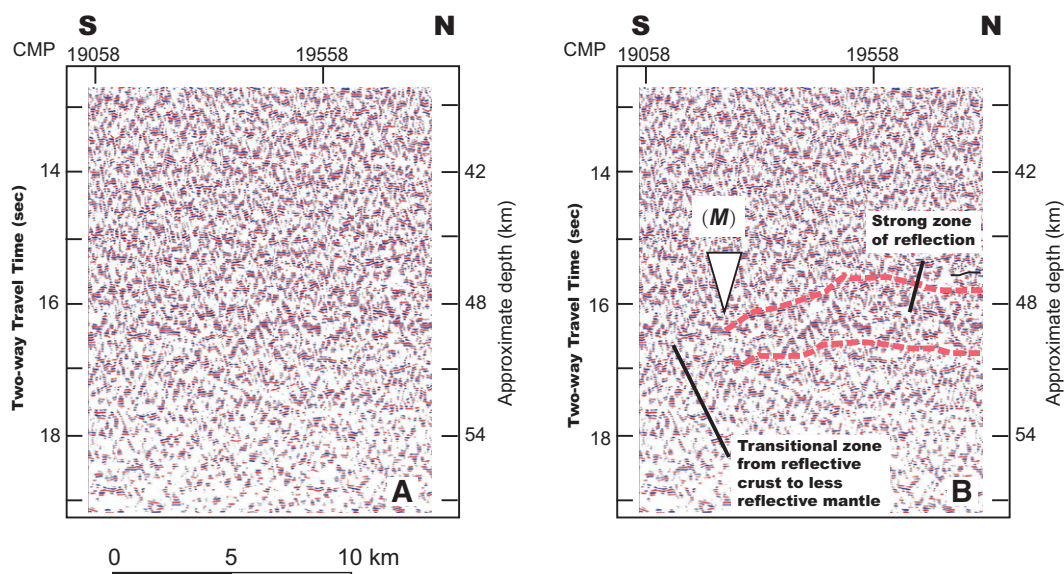


**Figure 5.** Close-up view of a portion of the reflection profile obtained from this study. See Figure 3A for location. (A) Uninterpreted and (B) interpreted seismic section. The close-up view shows a region where the Moho between the crust and the mantle is transitional. Also shown are the contrasts in the style of seismic reflectivity in the lower crust and upper mantle. The lower crust is characterized by reflectors that are <3 km in length, variably dipping, and disharmonic between curved reflectors. The reflectivity in the mantle is much weaker and is characterized by the presence of large regions of no reflection, shown white, which surround sparsely occurring and randomly dipping reflectors that are generally shorter than 100–200 m.

each reflector sequence, individual reflectors are spaced ~3–4 km vertically and extend laterally for 15–30 km before they are truncated by the seismically transparent regions associated with low seismic reflectivity (Fig. 3A). Some middle-crustal reflectors appear to be truncated and/or offset by faults (e.g., reflectors 5 and 6 in Fig. 3A), whereas others appear to be folded (e.g., reflectors 3 and 4 in Fig. 3A). The truncation and offsets of the middle-crustal reflectors allow the downward extrapolation of the Haiyuan and Tianjing faults (Fig. 3A), which is discussed later herein.

### Reflectors in the Upper Crust

Interpreting structures in the upper crust requires a detailed knowledge of surface geology. Although regional geologic maps at a scale of 1:1,000,000 or smaller are available along our seismic line (e.g., Pan et al., 2004), detailed structural geologic mapping is lacking. As a result, the basic information on the geometry and kinematics of many faults across our seismic lines is poorly known. Because of this, our analysis of upper-crustal structures focuses only on the structures that are well determined in the field and for which ages are well known based on the crosscutting relationships to the known stratigraphic units. In Figures 6, 7, and 8, we show interpreted upper-crustal structures associated with the Baiyin thrust, which places Proterozoic–Paleozoic strata over Cretaceous strata near our seismic line and cuts Cenozoic strata farther to the east (Fig. 2), the Haiyuan fault, which cuts Neogene and Quaternary strata and is seismically active (e.g., Burchfiel et al., 1991), and the Tianjing fault,

which has also been shown to be active in the Quaternary (Burchfiel et al., 1991; Gaudemer et al., 1995). The lithologic units assigned to the interpreted sections are extrapolated from the surface and divided sequentially according to the interpreted stratigraphic and structural relationships. Detailed geologic mapping, in association with interpreting detailed structures shown in our seismic-reflection profile, is ongoing, and the results of more detailed assignment of lithologic units and their ages in the interpreted cross sections are in preparation and will be presented elsewhere.

In general, upper-crustal reflectors are characterized by finely laminated layers and are interpreted as representing sedimentary strata. Upper-crustal deformation was determined from the structural geometry of the reflector sequences. For example, reflector sequence 3 in Figure 6A is truncated by faults, whereas reflector sequence 4 in Figure 6A is folded.

One prominent structure imaged in our seismic profile is the low-angle, south-dipping Baiyin fault (Figs. 2 and 6A). This fault branches off from the Haiyuan fault in the west and curves into a north-striking fault zone that cuts Neogene strata (Fig. 2). The south-dipping fault places Proterozoic to Lower Paleozoic strata over Upper Cretaceous strata directly east of our seismic line (Fig. 2). Although the fault is nearly parallel to the Haiyuan fault at the location where it intersects the seismic line, its overall strike is oblique to the Haiyuan fault (Fig. 2). Because the Baiyin fault merges with the Haiyuan fault in the west and cuts Cretaceous and Neogene strata in the east, it must be a Cenozoic structure that is kinematically linked with motion on the Haiyuan fault. This inference,

together with (1) its oblique geometry to the Haiyuan fault in map view and (2) its low-angle geometry imaged in our seismic profile in cross-section view, leads us to interpret the Baiyin fault to be a thrust fault. Unfortunately, there are no detailed kinematic studies on this fault, and thus our interpretation needs to be tested by future studies.

Following the interpretation that the Baiyin fault is a thrust, we constructed a balanced cross-section model (Figs. 6B and 6C) based on seismic data shown in Figure 6A. Based on the characteristics of reflectors and their similarities, we propose four correlative reflector sequences. Reflector 1 in Figure 6A is marked by closely spaced and finely laminated parallel reflectors. This reflector sequence is interpreted to be offset by a low-angle fault. Reflector 2 is also a strong reflector sequence that is thinner than the thickness of reflector sequence 1 and lies below it (Fig. 6A). This reflector sequence is highly discontinuous laterally and is interpreted to have been duplicated by faults, as shown in Figures 6B and 6C. Reflector sequence 3 lies structurally below reflector sequence 2 and is characterized by more widely spaced and thickly laminated reflectors when compared to reflector sequences 1 and 3 (Fig. 6A). Another key feature of reflector sequence 3 is the weak reflectivity directly above the reflector sequence, displaying a whitish appearance in the seismic-reflection profile (Fig. 6A). Reflector sequence 4 is expressed by short zones of strong parallel reflectors (Fig. 6A). Individual reflectors in the sequence are thicker than those in other reflector sequences, and there is an upward-decreasing gradient of reflectivity associated with this reflector sequence (Fig. 6A).

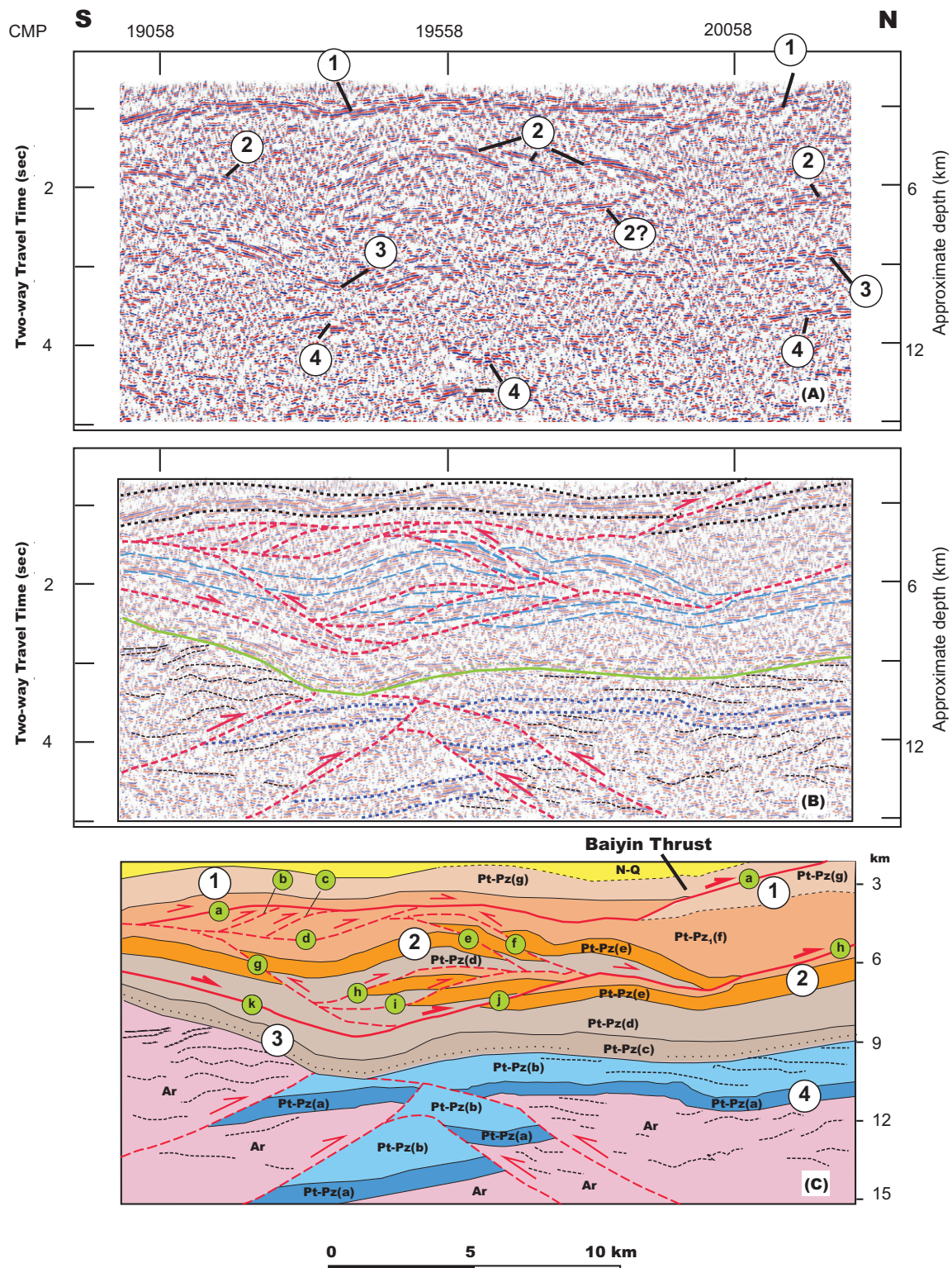
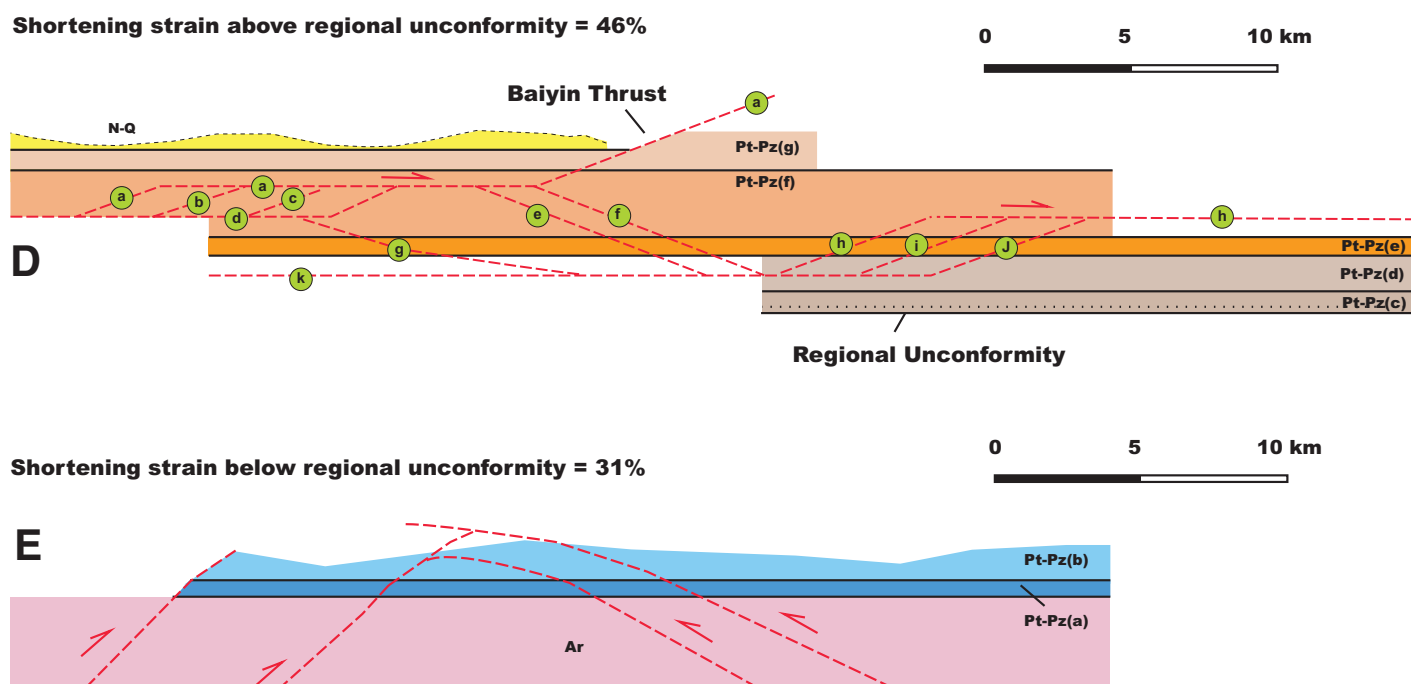


Figure 6. (A) A close-up view of upper-crustal structures from regional seismic profile obtained from this study. See Figure 3A for location. Also shown are major reflectors and reflector sequences labeled from 1 to 4. Reflectors with same numbers display seismic fabrics and are interpreted to represent the same layered geologic units. (B) Interpreted section showing inferred faults and geologic contacts superposed drawn on the seismic profile. (C) Cross section constructed based on the interpreted seismic profile in B, surface geology, and the thickness information from major lithologic units near the seismic profile. Lithologic units are interpreted based on thickness information of individual stratigraphic units in the area. Unit symbols are defined as follows: Ar—inferred Archean crystalline basement; Pt-Pz(a) to Pt-Pz(g)—Proterozoic to Paleozoic lithologic units inferred from the interpreted structural and stratigraphic relationships; N-Q—Neogene and Quaternary surficial deposits. (Continued on following page.)



**Figure 6 (continued).** (D) Restored cross section above the regional unconformity. Symbols of lithologic units are the same as in those C. (E) Restored cross section below the regional unconformity. Symbols of lithologic units are the same as in those C.

As the same reflector sequences are warped and vertically stacked on top of one another, we interpret their lateral discontinuity as resulting from crustal shortening. This interpretation leads to the construction of a balanced cross section shown in Figures 6B and 6C. Our cross section is restorable and thus presents a plausible solution to the interpretation of the seismic profile shown in Figure 6A. However, the cross section is not unique (e.g., Judge and Allmendinger, 2011). For example, our interpreted cross section shows an unconformity at the base of the Neoproterozoic strata, which is consistent with the field relationship in the region where Archean to Paleoproterozoic crystalline rocks are intruded by 750–1190 Ma plutons and are overlain by Neoproterozoic strata (Guo et al., 1999; Wan et al., 2001, 2003; H. Wang et al., 2007; Tung et al., 2012). However, the same feature could be interpreted as a thrust fault separating two styles of deformation above and below. The unconformity interpretation requires two phases of deformation, whereas the thrust interpretation does not. In addition, the unconformity interpretation requires less amount of shortening after the formation of the unconformity, while the thrust interpretation requires the development of contractional structures at two structural levels and thus much more shortening strain accommodated by these structures. In this study, we adopt the unconformity interpretation as shown

in Figure 6C to derive a minimum amount of shortening in the upper structural panel after the formation of the unconformity. The lack of thrusts cutting across the unconformity can be explained by the presence of a thrust décollement above the unconformity.

As stated in the introduction, all Cenozoic thrusts in the Qilian Shan region involve metamorphic basement rocks, and their cover strata were deformed during the early Paleozoic Qilian orogeny and Cenozoic formation of the northeastern Tibetan Plateau. Because of this deformation style and deformation history, the thin-skinned balanced cross-section methods that assume horizontal strata above a horizontal décollement are inappropriate in restoring the cross sections in this region. Rather, sections can only be balanced locally using a piecemeal bed-length balancing method as done in this study for restoring the cross section shown in Figure 6C. This approach yields ~46% of horizontal strain shortening above the interpreted unconformity (Fig. 6D). As the Baiyin thrust places Ordovician strata over Cretaceous strata, and its hanging wall consists of a syncline cored by Neogene–Quaternary strata (Fig. 6C), motion on the thrust likely occurred in the Cenozoic. The structures below the Baiyin thrust involve Proterozoic and Paleozoic rocks and potentially could be much older. However, as the Baiyin thrust is kinematically linked with the structures below via several duplexes, we interpret this estimated shortening

above the regional unconformity to have been induced entirely in the Cenozoic.

In contrast to the large shortening strain above the unconformity, restoring the cross section below the inferred unconformity indicates a shortening strain of ~31% (Fig. 6E). Although most of the strain must have been accumulated prior to the deposition of interpreted Proterozoic strata, the involved thrusts may have been reactivated afterwards, as the overlying unconformity is folded, and the fold geometry appears to be linked with motion below via fault-propagation folding (Figs. 6C and 6E).

#### Downward Extrapolation of the Haiyuan and Tianjing Faults and the Depth of Cenozoic Detachment below the Qilian Shan

Although the Haiyuan and Tianjing faults are well defined by their surface morphology (Fig. 1), extrapolating their downward extents is not straightforward. The main approach adopted in this study is to establish successive termination points of prominent and horizontally continuous reflectors downward starting from the surface traces of the fault (Fig. 3) (also see C.S. Wang et al., 2011). We also use the boundaries of the seismically transparent regions as offset markers. Using this approach, we interpret the downward projection of the Haiyuan fault to follow the termination points of reflector sequences 2, 3, 4, 5, 6, and 7 in Figure

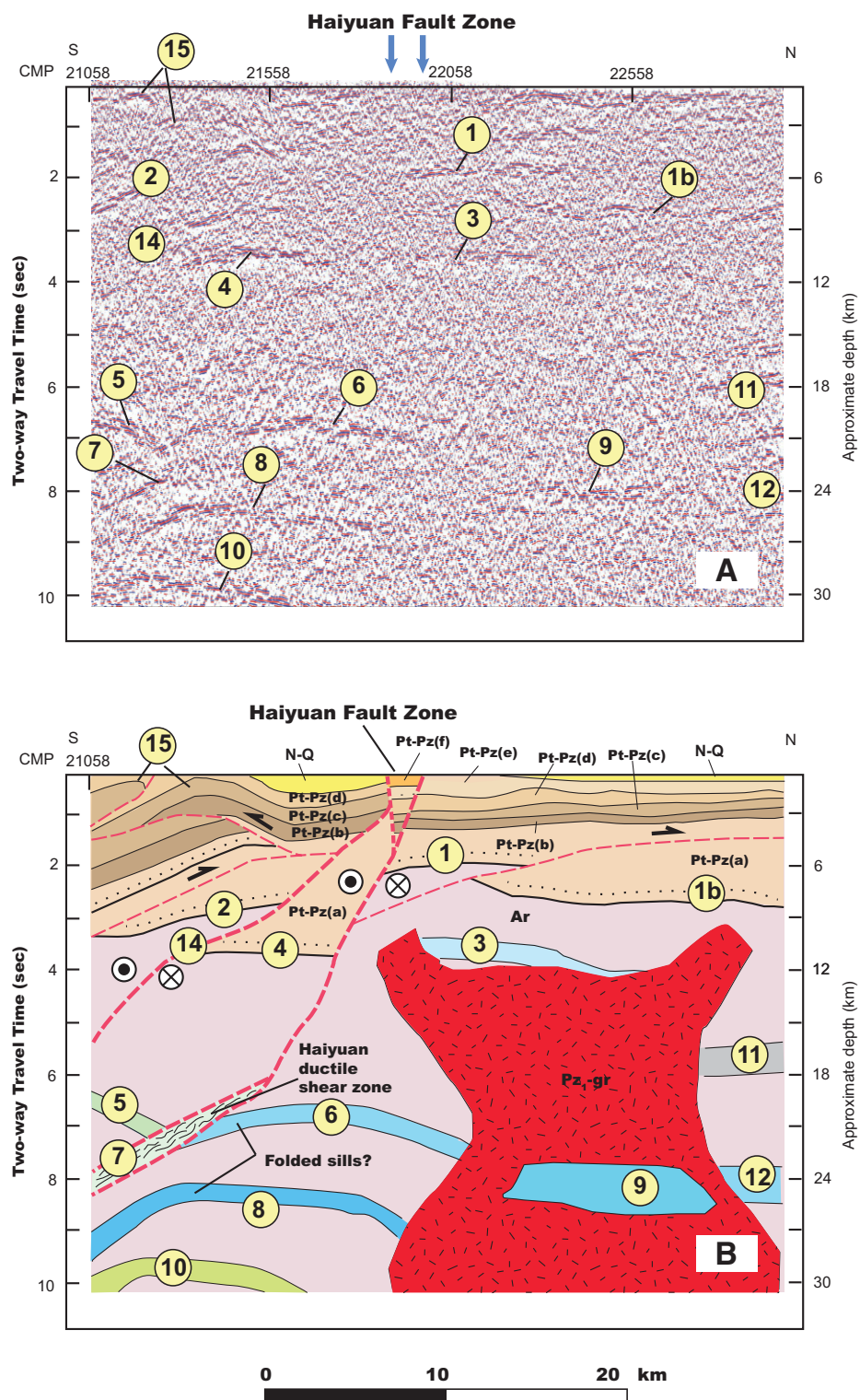


**Figure 7.** (A) Close-up view of the upper-crustal structure of the Haiyuan fault zone. Major reflectors labeled from 1 to 14 constrain the possible vertical extent of the Haiyuan fault zone in the seismic profile. (B) Interpreted geologic section based on relationships shown in A. Lithologic units: Ar—*inferred Archean crystalline basement*; Pt-Pz(a) to Pt-Pz(f)—*Proterozoic and Paleozoic lithologic units inferred from the interpreted structural and stratigraphic relationships*; N-Q—*Neogene and Quaternary surficial deposits*.

3A. Similarly, we interpret the projection of the Tianjing fault to follow the termination points of reflectors in reflector sequence 10 in Figure 3A.

In our interpreted seismic profile, the two branches of the Haiyuan fault zone dip steeply at  $60^{\circ}$ – $70^{\circ}$  to the south in the uppermost crust and merge with each other at a depth of 8–10 km (Fig. 3). As the reflectors directly below the surface fault trace are discontinuous, we interpret the fault zone to split from the surface downward into two branches. Having the fault traces follow the reflector termination points requires the fault to dip at a shallower angle of  $\sim 30^{\circ}$  to the south, cutting through the lower portion of the upper crust and most of the middle crust (i.e., from 10 km to 40 km) (Fig. 3). As the lower crust is seismically transparent, we are unable to locate the trace of the Haiyuan fault through the lower crust.

In order to unravel the detailed structural relationship between the Haiyuan fault and its adjacent structures, we analyzed in detail the seismic image near the fault in the upper crust (Fig. 7A). Similar to the detailed seismic profile shown in Figure 6A, the upper-crustal reflectors are characterized by finely laminated layers interpreted to represent sedimentary strata. Like in Figure 6, a boundary between finely laminated reflectors and more widely spaced strong reflectors can be established, which is interpreted as the regional unconformity between crystalline basement rocks (possibly Archean to Mesoproterozoic in age) below and Neoproterozoic strata above (Fig. 7B). A large, seismically transparent region in the cross section (Fig. 7A) is interpreted as an early Paleozoic plutonic body (Fig. 7B).

Due to the presence of strike-slip/oblique-slip faults in the cross section, it is impossible to estimate the total shortening across the section as done for Figure 6. This is because offsets along the strike-slip faults would produce apparent separations that are unrelated to motion on the strike-slip faults (cf., Gaudemer et al., 1995). If we only restore the folded Carboniferous–Permian strata, we obtain  $\sim 8$  km shortening from the 40-km-long section. This yields  $\sim 17\%$  shortening accumulated after the deposition of Carboniferous and Permian strata. This would be a maximum estimate of Cenozoic shortening across the section shown in Figure 7 without considering the role of oblique slip across the Haiyuan fault.

The geometry of the Tianjing fault is equally complex as determined by the truncation of prominent reflectors (Fig. 3). The fault zone is nearly vertical in the uppermost part of the seismic section and dips steeply at  $\sim 60^{\circ}$ – $70^{\circ}$  to the north at depths of 6–15 km. The fault zone splits into two branches between 15 km and 40 km.

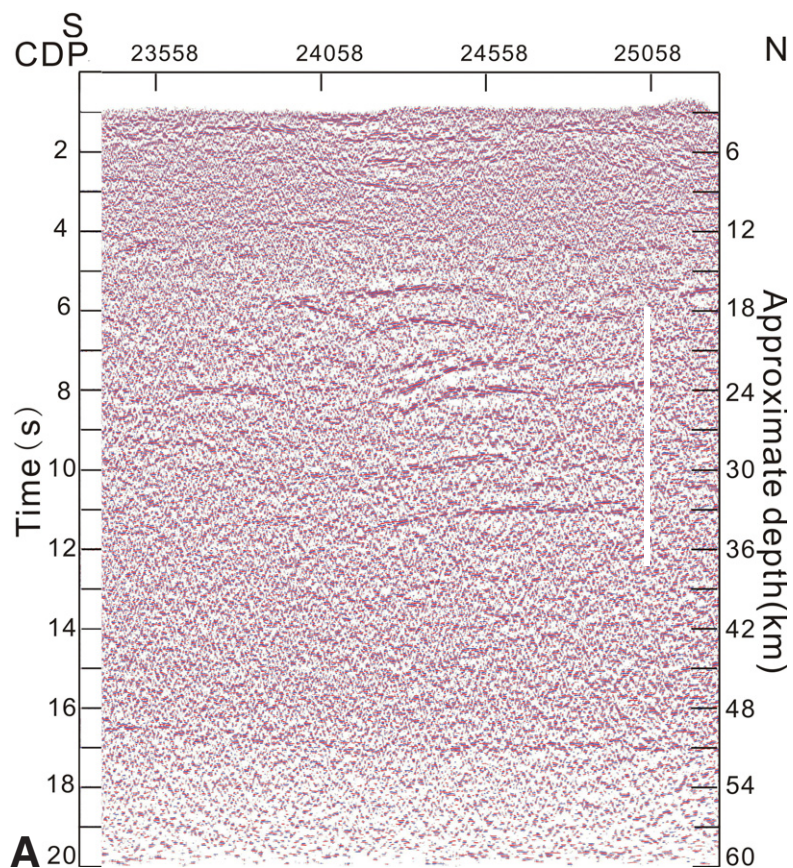
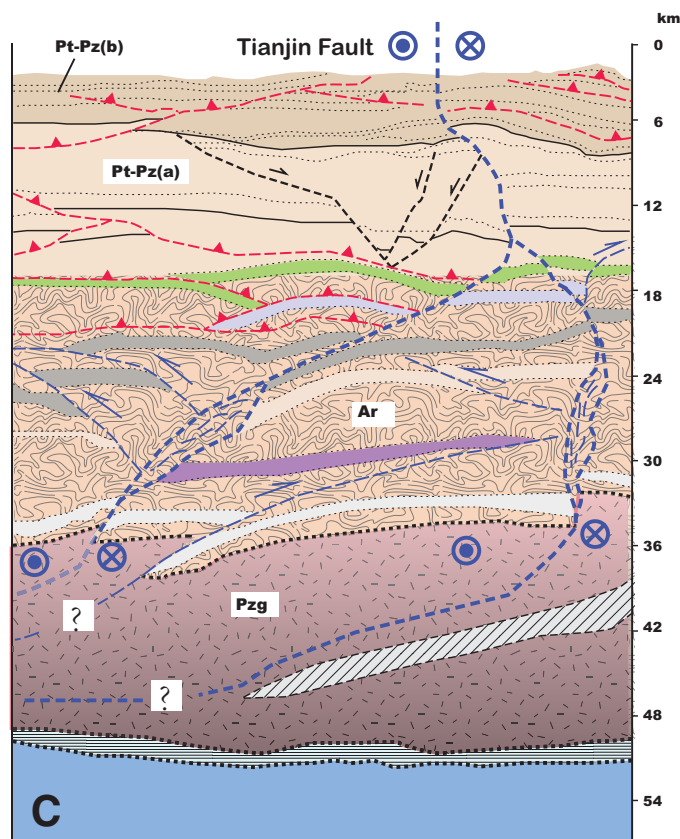
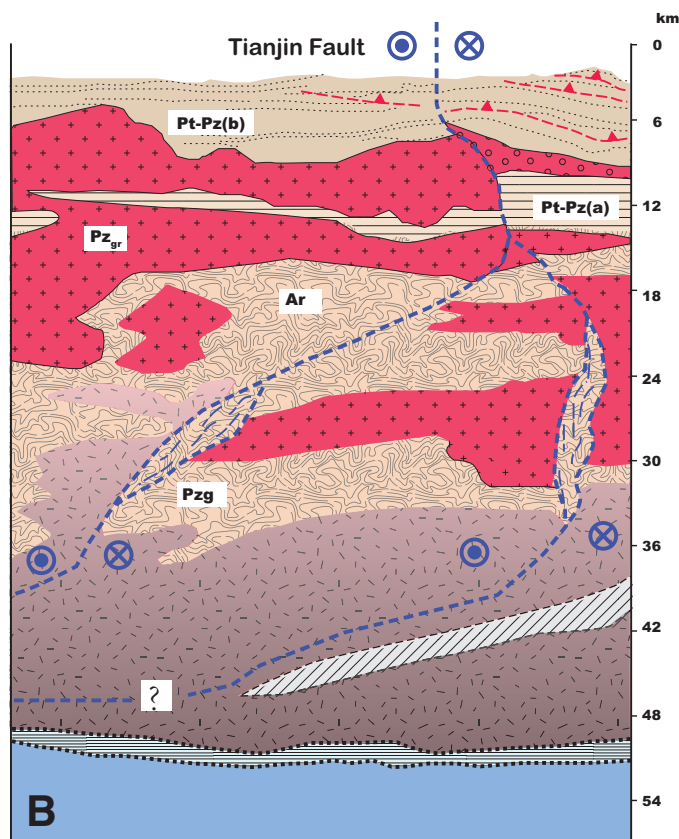


Figure 8. (A) Uninterpreted seismic-reflection profile with location shown in Figure 3A. (B) The highly reflective regions and reflectors in the middle crust are interpreted as Archean gneissic basement (Ar) that contains many strong reflectors. The reflectors are truncated by seismically transparent regions interpreted as early Paleozoic granitic intrusions (unit Pzgr) with irregular shapes. The seismically transparent lower crust and its immediate upward extension in the middle crust are interpreted as dominantly intermediate plutons based on the seismic speed and its interpretation by M.J. Liu et al. (2006). Lithologic units: Ar—inferred Archean crystalline basement; Pt-Pz(a) and Pt-Pz(b)—Proterozoic and Paleozoic sedimentary and volcanic units inferred from the interpreted structural and stratigraphic relationships; N-Q—Neogene and Quaternary surficial deposits. (C) The highly reflected middle crust is interpreted to represent crystalline basement containing subhorizontal reflectors. Instead of being truncated by plutonic rocks as shown in B, the termination of reflectors is interpreted to have resulted from faulting. The strong reflectors may represent individual compositional layers within the gneiss unit. Similar to interpretation in B, the seismically transparent lower crust is interpreted as batholith roots of the early Paleozoic Qilian arc with an intermediate composition.



While the northern branch is mostly vertical, the southern branch dips at  $\sim 25^{\circ}$ – $30^{\circ}$  to the south across the middle crust. The presence of a south-dipping and continuous reflector below the northern branch (i.e., reflector 12 in Figs. 3B and 3C) requires that the fault becomes a south-dipping shear zone in the lower crust. Since the Moho directly below the projected trace of the Tianjing fault in the lower crust is not offset, the fault likely terminates before reaching the Moho and extends below the base of the highly reflective middle crust. That is, the rather flat décollement required to terminate the strike-slip faults above likely lies below a depth of  $\sim 40$  km, i.e., much deeper than the inferred décollement depth of  $\sim 20$  km by Gaudemer et al. (1995). The lack of continuous and long ( $>3$  km) reflectors in the lower crust makes the exact position of this inferred décollement in the lower crust uncertain.

## DISCUSSION

Our analysis of the seismic-reflection profile leads to the following first-order observations. First, the upper crust is characterized by finely laminated seismic reflectors that can be correlated with exposed Proterozoic and Phanerozoic strata (e.g., reflectors 1, 2, 3, and 4 in Fig. 6A). Second, the Haiyuan and Tianjing faults can be confidently extrapolated across the upper crust and parts of the middle crust, but their traces through the lower crust and the uppermost mantle are uncertain. Third, the middle crust is characterized by highly reflective sequences that are truncated by seismically transparent regions. The latter can be extended continuously throughout the lower crust. Finally, the Moho changes its character from a narrow (hundreds of meters) zone of high reflectivity to a wide (4–6 km) zone with an abrupt decrease in reflectivity with depth. These observations have important implications for the magnitude and mode of Cenozoic deformation responsible for the development of the northeastern Tibetan Plateau, the vertical extent of major strike-slip faults in the lithosphere, the early Paleozoic development of the Qilian orogen, and the nature of the Moho below our seismic survey line. We discuss these points in turn next.

### Magnitude of Cenozoic Shortening

According to the current knowledge of the regional tectonic history (e.g., Yin et al., 2007a), the Qilian Shan region experienced an arc-continent collision in the Devonian, followed first by shallow-marine deposition from Carboniferous to Triassic and then Jurassic–Cretaceous intracontinental extension. This pre-Cenozoic history means that any contractional structures

involving Carboniferous and younger strata most likely have been formed in the Cenozoic. If these strata were not tilted in the Mesozoic during extension, restoring their bed lengths would yield the shortening magnitude for Cenozoic deformation. Based on this argument, the  $\sim 17\%$  shortening strain estimated from restoring folded Carboniferous and Permian strata in Figure 7B may have all resulted from Cenozoic deformation. We admit that this estimate is highly uncertain, and it is equally possible that all the estimated shortening strain was accumulated prior to the Cenozoic, and thus the estimated  $\sim 17\%$  shortening strain is a maximum possible value for Cenozoic deformation.

A more robust estimate of Cenozoic shortening strain comes from balancing a cross section across the Baiyin thrust system shown in Figure 6. This led to an estimated 46% shortening strain likely accumulated all in the Cenozoic (Fig. 6). This strain is significantly higher than  $\sim 10\%$  strain estimated across the west and east sides of Xining Basin south of our study area (Lease et al., 2012b) (Fig. 1). The difference may be explained by a heterogeneous distribution of Cenozoic strain across the northeastern Tibetan Plateau, which is consistent with the variable topography in the region (Fig. 1C).

It is important to note that shortening strains estimated from surface geology alone may grossly underestimate the true crustal shortening strain. For example, in Figure 6, the most dominant Cenozoic structures are blind thrusts that cannot be detected by surface mapping. This ambiguity highlights the importance of subsurface data such as high-resolution seismic-reflection profiles presented here for constructing more plausible and geologically testable balanced cross-section models (e.g., Yin et al., 2007b, 2010; Judge and Allmendinger, 2011). It also reiterates the possibility that shortening estimates based on surface geology alone may at best be regarded as lower bounds due to potential neglect of hidden décollements and duplex systems, a prominent problem in studies of the Cenozoic Himalayan–Tibetan orogen (e.g., Yin et al., 2008a, 2008b, 2010). In addition to these issues, strain may be transferred from upper crust to the middle and lower crust via horizontal detachment shear zones. Under such conditions, regions with little upper-crustal deformation could have experienced significant middle- and lower-crustal deformation (e.g., C.S. Wang et al., 2011).

### Vertical Extent and Structural Nature of Major Cenozoic Strike-Slip Faults

Gaudemer et al. (1995) inferred the Haiyuan fault to flatten southward at a depth of 20 km

into a thrust décollement that dips a few degrees to the south. The interpreted geometry of the Haiyuan fault from our study differs from this interpretation in that the fault zone cuts across the whole middle crust from 15 to 40 km with a southward dip of  $\sim 30^{\circ}$  (Figs. 3B and 3C). Although it is clear that the Haiyuan fault does not cut and offset the Moho, it is not clear how the Haiyuan fault terminates in the lower crust due to a lack of reflectors at this depth. Several lines of evidence argue that the fault flattens into a subhorizontal décollement in the lower crust. First, the northern branch of the Tianjing fault flattens into a décollement at the transition zone between the middle and lower crust. Second, the north-dipping ductile thrust zone offsetting the Moho also appears to terminate at a décollement zone at the top of the lower crust or base of the middle crust. Third, if the Haiyuan fault zone cuts across the lower crust, one would expect the fault zone to form a prominent reflector defined by the shear fabrics, which is not seen. Because of these arguments, we favor the model shown in Figure 3C, in which the Haiyuan and Tianjing faults and the Moho-offsetting thrust zone all merge into a décollement at the base of the middle crust or within the lower crust. This model implies that the mantle lithosphere is at least locally deformed via thrusting, possibly due to southward wedging of North China into Tibet in across-section view. Although this interpretation of the kinematics is similar to the wedge tectonic model of Yin (2010) for the development of the eastern Tibetan Plateau and its foreland, the strike-slip motion parallel to the plateau margin of northeastern Tibet may be more dominant than strike-slip faulting parallel to the plateau margin of eastern Tibet.

Burchfiel et al. (1991) and Zhang et al. (1991) established the geometric linkage between left-slip motion on the east-striking Haiyuan fault system and north-trending Liupan Shan thrust belt at its eastern end. Burchfiel et al. (1989) argued that the Qilian Shan thrust belt at the western end of the Haiyuan fault zone soles into a décollement in the middle crust. Our finding that the Haiyuan and Tianjing faults sole into a flat décollement in the lower crust is conceptually similar to the proposal by Burchfiel et al. (1989), although its position lies at a deeper structural level. Our finding that the Haiyuan fault does not cut across the mantle suggests that the structure may have served as a lateral ramp of an east-directed crustal-scale thrust system, with the Liupan Shan thrust belt as its surface expression and the lower-crustal décollement as its main sliding surface below much of the northeastern Tibetan Plateau. The Tianjing fault may have acted the same way as the Haiyuan fault and has acted as a strike-slip transfer fault

soling downward into the lower-crustal décollement and linking in the east with the Liupan Shan thrust belt. The corrugated fault geometry of the Tianjing fault shown in Figures 3B and 3C is consistent with the surface observations and supports the interpretation that the fault is a strike-slip structure (Burchfiel et al., 1991).

Our inferred décollement terminating the Haiyuan and Tianjing fault zones should display a zone of high reflectivity at the top of the lower crust. Evidence for such a feature is lacking. There are two possible explanations. First, the seismic velocity contrast across the inferred shear-zone slip surfaces is too small to show reflectivity in the seismic profile. Second, the termination zone of the strike-slip faults in the lower crust is not a single and concentrated shear zone. Rather, the strike-slip slip faults have multiple strands that may have been terminated in multiple subhorizontal shear zones bounding highly deformable regions in the lower crust. In other words, motion on the strike-slip was absorbed by diffuse ductile deformation without formation of a clearly defined décollement shear zone.

### Strong Reflectors and Seismically Transparent Regions in the Middle Crust

Two end-member interpretations of the nature of the middle-crustal reflectors are shown in Figure 8 (see Fig. 3A for location). In Figure 8A, the prominent reflectors in the middle crust are interpreted as Archean gneissic basement ( $Ar_{gn}$ ), which contains strong reflectors that may have been induced by subhorizontal compositional zonation. The strong subhorizontal reflectors are truncated by seismically transparent regions in the middle and lower parts of the upper crust (i.e., at depths of 6–16 km in Fig. 8B), which are interpreted as early Paleozoic granitic intrusions (unit  $Pz_{gr}$ ) that display irregular shape. The seismically transparent lower crust and its immediate upward extension in the middle crust are interpreted as plutons with an intermediate composition ( $Pz_{gr}$ ) at the base of the early Paleozoic Qilian arc, following the interpretation of M.J. Liu et al. (2006).

In Figure 8B, both the prominent reflectors and transparent regions in the middle crust are interpreted as representing Archean crystalline basement rocks. In this interpretation, the termination of reflectors is interpreted to have resulted from fault offsets. The strong reflectors in the interpreted basement may represent individual compositional layers within the gneissic unit, whereas the transparent regions may represent Mesoproterozoic intrusions (not shown in Fig. 8B) emplaced before the deposition of the interpreted Neoproterozoic strata based on

regional stratigraphic relationships and ages of Precambrian plutons (Tseng et al., 2006; Xue et al., 2009; Tung et al., 2007a, 2007b). A special feature of this interpretation is that by removing an interpreted plutonic complex in the upper crust, the irregular geometry of reflectors in the interpreted Proterozoic strata may be interpreted as a result of normal faulting that occurred prior to deposition of the Paleozoic strata (Fig. 8B). Additionally, the arrangement of strong reflectors in the middle crust could be explained by the development of ductile contractional shear zones (Fig. 8B).

The third possibility, not shown in Figure 8, is that the reflectors may represent metasediments that were emplaced tectonically via flat subduction of an oceanic plate that carried and accreted a large volume of sediments below the upper crust of the overriding plate (e.g., Kapp et al., 2000). The emplaced metasediments were later cut by the younger plutons. Although this model also predicts a continental-crust composition in the middle crust, the provenance of materials is not native to North China, but from materials originally deposited in an oceanic basin (e.g., the Qilian ocean[s] to the south of North China) that was closed in the early Paleozoic. This prediction may be tested in the future by systematic examination of xenoliths in the Phanerozoic igneous rocks. Again, as the subhorizontal reflectors interpreted to represent foliation created by underplating processes are truncated by seismically transparent regions, it requires a younger geologic event, interpreted here as plutonic emplacement, during the construction of the early Paleozoic Qilian arc.

M.J. Liu et al. (2006) showed that the seismic speeds of the middle and lower crust in our study area correspond to an intermediate rock composition based on seismic-refraction data. This composition favors ductile flow in the middle and lower crust for a normal thermal gradient (e.g., Brace and Kohlstedt, 1980). Because of this, it is possible that the seismically transparent regions in our section represent rising ductile lower-crustal material emplaced into the middle crust in the Cenozoic as the result of a lateral pressure gradient imposed by the high-plateau elevation to the south. If this processes occurred in the Cenozoic, the lateral dimension of the seismically transparent regions in the middle crust on the order of 20–50 km and the 10–20 km upward motion tracing from the lower-crustal source regions to their current middle-crustal position would require highly irregularly shaped uplifts with great reliefs in the Cenozoic in the study area. The rather smooth topography in the region where the seismically transparent bodies are present is not consistent with this hypothesis.

Among the four possible interpretations mentioned here for the origin of the middle-crustal seismic fabrics and seismically transparent regions, we find the first interpretation—that foliated basement rocks were intruded by early Paleozoic plutons—to be most consistent with the surface geology and regional tectonic setting. Specifically, the P-wave seismic velocity (M.J. Liu et al., 2006) and transparent fabrics in the lower crust may be explained as batholith roots of the Qilian arc with an intermediate composition (Fig. 8A). In addition, the lack of through-going subhorizontal reflectors and the preservation of irregular subvertical contacts between subhorizontal reflectors and seismically transparent regions (interpreted as early Paleozoic plutons) preclude midcrustal channel flow in the Cenozoic below the study area.

### Deformation in the Lower Crust

It is unclear from our seismic data whether channel flow occurred in the lower crust during the Cenozoic. This is because we are unable to quantify the mode and magnitude of deformation in the lower crust as it appears seismically transparent and lacks reflectors that can be used as strain markers. In one interpretation, the seismically transparent lower crust represents outward (northward)–flowing ductile materials from the interior of the high plateau to the low-altitude plateau margin in the Cenozoic as proposed in Clark and Royden (2000). If lower-crustal material transport was accommodated by laminar flow (Bird, 1991; Clark and Royden, 2000), two through-going shear zones with opposite senses of shear should bound the unidirectional-flow channel (Fig. 9A). Specifically, the intensity of shear-zone fabrics as measured by preferred mineral-shape alignments should increase toward the channel walls, decrease toward the channel interior, and completely disappear at the channel axis where shear strain vanishes (Fig. 9A). Such anticipated fabric development and strain distribution have been documented in the Cenozoic Himalayan orogen, where the middle and locally lower crust were extruded outward along the two parallel crustal-scale shear zones with opposite senses of shear, that is, the south-directed Main Central thrust below and the north-directed South Tibet detachment above (e.g., Grujic et al., 1996; Webb et al., 2011). Shear-generated subhorizontal foliation by lower-crustal channel flow in our study area should be detectable by reflection seismology as strong subhorizontal reflectors if they were generated by a similar process as that inferred for the development of the Himalaya (e.g., Nelson et al., 1996). The lack of observed reflector sequences at the top and base of the

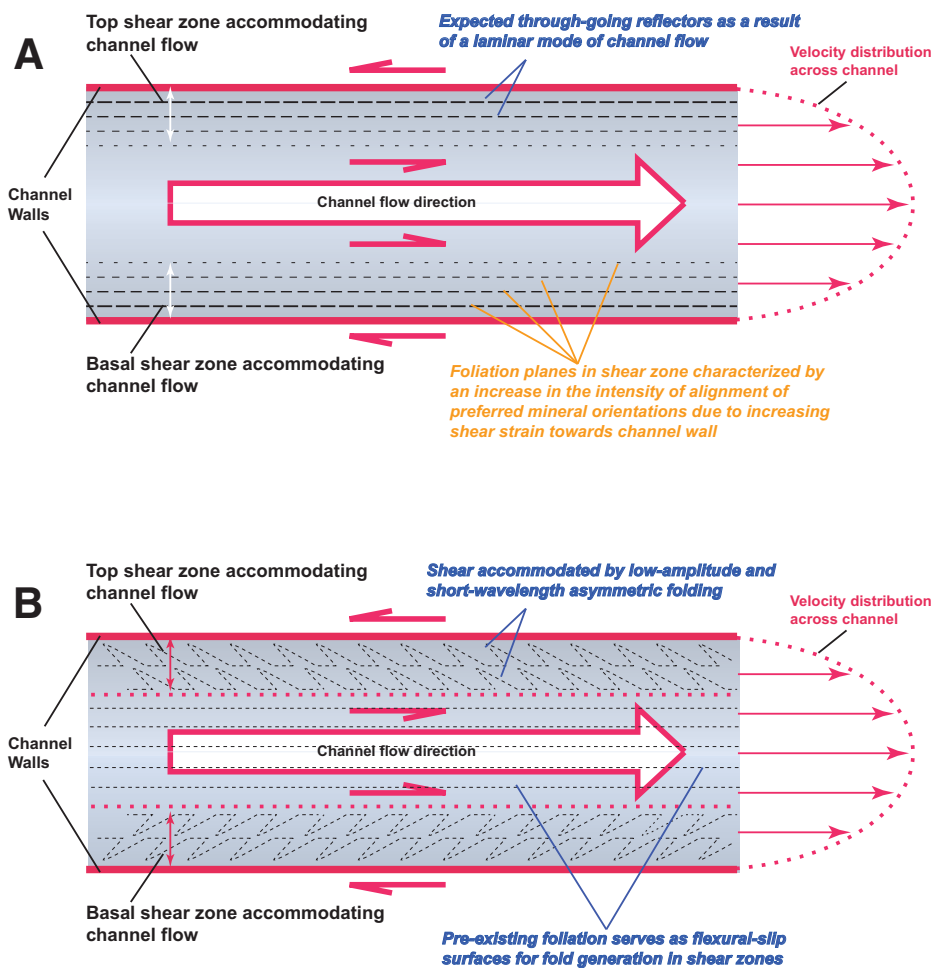


**Figure 9.** Two modes of lateral transport of ductile material in the lower crust. (A) A laminar mode of flow transport in a lower-crustal channel. Two shear zones with opposite senses of shear are developed above and below the flowing channel. The shear zones comprise through-going shear-foliation surfaces and should be detectable by reflection seismology as strong reflectors. (B) The lateral flow of lower-crustal material is accommodated by shear zone development above and below the flowing channel. However, the shear zones are characterized by the formation of short-wavelength and low-amplitude folds that are not detectable by seismic-reflection seismology performed in this study due to its limited resolution. Note that in order to have asymmetric folds develop in the shear zones, preexisting layering prior to channel flow is required in the lower crust.

lower crust is inconsistent with the laminar mode of channel flow in the lower crust.

Alternatively, the lateral transport of ductile lower-crustal material could have been accommodated by the development of shear zones without the formation of through-going zones of subhorizontal shear foliation (Fig. 9B). That is, shear deformation at the bounding zones of a unidirectional-flow channel could have been accommodated by the development of low-amplitude and short-wavelength (less than a few kilometers at the resolution of our seismic-reflection images) asymmetric folds. Such non-coaxial deformation is commonly associated with formation of secondary parasitic folds within a larger flexural-slip fold. A key condi-

tion for this mode of shear-zone development is the presence of preexisting layers, which serve as flexural-slip surfaces. The lack of reflectors within the interior of the lower crust (i.e., regions that should not have been affected by shearing during channel flow) appears inconsistent with this model. However, we cannot rule out the possibility that the composition of the lower crust is highly uniform and the velocity contrasts across these preexisting foliation surfaces are too small to be detectable. This mechanism may also explain the lack of seismic expression of the inferred décollement in the lower crust that is interpreted in this study to terminate the left-slip Haiyuan and Tianjing faults (see earlier discussion).

We note that the seismically transparent regions extend continuously upward from the lower crust and link directly with the seismically transparent regions in the middle crust in the seismic profile (Fig. 3A). This relationship requires a similar origin of the seismically transparent regions in the middle and lower crust. As argued earlier herein, i.e., that the seismically transparent regions in the middle crust most likely represent early Paleozoic plutons in the Qilian arc, we favor an interpretation that the seismically transparent lower crust represents the base of the same arc comprising intrusive rocks that lack internal structural fabrics.

### Cause for Changes in Seismic Fabrics along the Moho Zone

There are at least four possible explanations for the observed lateral variation of seismic fabrics along the Moho zone: (1) It represents a mantle suture linking with the north-dipping South Qilian suture zone, (2) it represents a mantle suture linking with the south-dipping North Qilian suture zone, (3) it results from strike-slip faulting juxtaposing different lithospheric structures and thus different mantle zones, and (4) it is an inherited feature within a single continental block such as the North China craton.

Interpreting the lateral variation of the Moho zone as the result of north-dipping subduction would require the presence of a major north-dipping reflector zone in the lower crust, which is not observed (Fig. 3). Similarly, interpreting a south-dipping subduction across the Moho zone would require the presence of a south-dipping reflector zone in the lower crust that is also not observed (Fig. 3). In principle, the lack of through-going dipping reflectors as required by these interpretations could have resulted from late tectonic and/or magmatic modification. One such process is Mesozoic extension in northern Tibet (e.g., Chen et al., 2003). However, since its magnitude is rather small (i.e., no exposed middle-crustal rocks in any of the known normal faults in the Qilian Shan and its foreland region), its occurrence is highly localized, and, most importantly, it was not associated with coeval and widespread igneous activity (e.g., Chen et al., 2003), this tectonic event does not appear to be an adequate solution to the problem. As mentioned already, Cenozoic lower-crustal channel flow does not seem to be a viable mechanism either. Because of the issues with these explanations, we favor an interpretation that partial melting of the lower crust, which is expressed by the emplacement of A-type granites in the region during the collision of the early Paleozoic Qilian orogen and the North China craton (e.g., Gehrels et al., 2003a, 2003b), may

have led to the elimination of the projected suture zones.

It is possible that motion on the Haiyuan fault could have juxtaposed different lithospheric sections of northern Tibet against each other (Fig. 3C). However, connecting the extrapolated trace of the Haiyuan fault with the Moho transition point M in Figure 3A is difficult, as its inferred position in the lower crust is completely unconstrained from our seismic data. Our preferred interpretation is that the lateral transition of seismic fabrics in the Moho zone was either inherited from the ancient structures of the North China craton or is the result of laterally inhomogeneous mixing of the mantle and crustal materials during construction of the early Paleozoic Qilian arc.

## CONCLUSIONS

The principal conclusions of our study are summarized here.

(1) The Moho is broadly warped and defined as a zone of high reflectivity with a thickness varying from a few hundreds of meters to 6 km. The locally thickened Moho zone can be explained by either offsets by north-dipping ductile thrusts (favoured), or localized magmatism, or distributed ductile shortening. A transition occurs from a sharply defined Moho to a diffusive Moho in the seismic profile over a distance of  $<2\text{--}3$  km. The origin of this transition zone is unknown.

(2) The reflectivity of the lower crust in our seismic profile is characterized by short ( $<3$  km), poorly organized, and disharmonic reflectors. As a result, the lower crust in the seismic profile appears to be transparent and lacks traceable seismic reflectors that are indicative of the mode of lower-crustal deformation. Because the lower crust in the study area has a P-wave velocity of  $\sim 6.8$  km/s and is located within the early Paleozoic Qilian arc, we interpret the seismically transparent lower crust to represent the intrusive rocks with an intermediate composition at the base of the arc.

(3) The middle crust in the seismic profile is dominated by isolated zones of subhorizontal and upward-warped reflectors that are truncated by seismically transparent regions. The latter are geometrically linked with the seismically transparent lower crust and thus are interpreted to represent arc plutons of the early Paleozoic Qilian arc. The subhorizontal reflectors represent structural and/or compositional layering of gneissic basement rocks of the North China lithosphere upon which the Qilian arc was constructed.

(4) Bed-length balancing of a segment of the seismic profile indicates that the upper-crustal shortening strain may reach 46% locally, which is significantly higher than the  $\sim 10\%$  shortening strain estimated by a previous study directly

west of our study area based on constraints from surface geology alone. We attribute this discrepancy to both spatial variability of strain in the region and the inability to recognize blind structures by surface mapping alone.

(5) Major transpressional structures (i.e., the Haiyuan and Tianjing faults) display complex geometry in the seismic profile, characterized by multiple strands cutting through the middle crust. The lack of continuous reflectors  $>3$  km in the lower crust and locally large thickness variations of the Moho zone (up to 6 km) make it uncertain if the transpressional faults cut across the lower crust and offset the Moho, or terminate at a subhorizontal décollement zone at the base of the middle crust.

## ACKNOWLEDGMENTS

We thank Clark Burchfiel, science editor Arlo B. Weil, Richard Lease, and an anonymous reviewer for their critical comments and constructive suggestions. This study was financed jointly by the SinoProbe Project (Sinoprobe-02) and the National Natural Science Foundation of China (no. 40830316). We are grateful to Dong-Ding Huang and his colleagues from Geophysical Exploration Division of the Huadong Petroleum Bureau for collecting high-quality seismic-reflection field data. We also thank Beijing Petrosound Geoservice, Ltd., for their able assistance in processing the seismic data. An Yin thanks the Tectonic Program of the U.S. National Science Foundation for supporting his research in Tibet and the Himalaya. His work has also been supported by the SinoProbe Project.

## REFERENCES CITED

- Bian, Q., Gao, S., Li, D., Ye, Z., Chang, C., and Luo, X., 2001, A study of the Kunlun-Qilian-Qinling suture system: *Acta Geologica Sinica—English Edition*, v. 75, p. 364–374.
- Bird, P., 1991, Lateral extrusion of lower crust from under high topography, in the isostatic limit: *Journal of Geophysical Research*, v. 96, p. 10,275–10,286, doi:10.1029/91JB00370.
- Brace, W.F., and Kohlstedt, D.L., 1980, Limits on lithospheric stress imposed by laboratory experiments: *Journal of Geophysical Research*, v. 85, p. 6248–6252.
- Burchfiel, B.C., Quidong, D., Molnar, P., Royden, L., Yipeng, W., Peizhen, Z., and Weiqi, Z., 1989, Intracrustal detachment within zones of continental deformation: *Geology*, v. 17, p. 748–752, doi:10.1130/0091-7613(1989)017<0448:IDWZ OC>2.3.CO;2.
- Burchfiel, B.C., Zhang, P., Wang, Y., Zhang, W., Song, F., Deng, Q., Molnar, P., and Royden, L., 1991, Geology of the Haiyuan fault zone, Ningxia-Hui Autonomous Region, China, and its relation to the evolution of the northeastern margin of the Tibetan Plateau: *Tectonics*, v. 10, p. 1091–1110, doi:10.1029/90TC02685.
- Chen, J., Xue, X., Wang, H., Wang, Z., Zheng, Z., Wang, C., and Li, P., 2008a, LA-ICPMS zircon U-Pb dating of Tangzang quartz-diorite pluton in the west segment of North Qinling Mountains and its tectonic significance: *Geoscience*, v. 22, p. 45–52.
- Chen, J., Xu, X., Zeng, Z., Xiao, L., Wang, H., Wang, Z., and Xiao, S., 2008b, Geochemical characters and LA-ICPMS zircon U-Pb dating constraints on the petrogenesis and tectonic setting of the Shichuan intrusion, east segment of the Central Qilian, NW China: *Acta Petrologica Sinica*, v. 24, p. 841–854.
- Chen, X., Yin, A., Gehrels, G.E., Cowgill, E.S., Grove, M., Harrison, T.M., and Wang, X.-F., 2003, Two phases of Mesozoic north-south extension in the eastern Altyn Tagh range, northern Tibetan Plateau: *Tectonics*, v. 22, 1053, doi:10.1029/2001TC001336.
- Clark, M.K., and Royden, L.H., 2000, Topographic ooze: Building the eastern margin of Tibet by lower crustal flow: *Geology*, v. 28, p. 703–706, doi:10.1130/0091-7613(2000)28<703:TOBTEM>2.0.CO;2.

- Clark, M.K., Farley, K.A., Zheng, D., Wang, Z., and Duvall, A.R., 2010, Early Cenozoic faulting of the northern Tibetan Plateau margin from apatite (U-Th)/He ages: *Earth and Planetary Science Letters*, v. 296, p. 78–88, doi:10.1016/j.epsl.2010.04.051.
- Cowgill, E., Yin, A., Harrison, T.M., and Wang, X.F., 2003, Reconstruction of the Altyn Tagh fault based on U-Pb geochronology: Role of back thrusts, mantle sutures, and heterogeneous crustal strength in forming the Tibetan Plateau: *Journal of Geophysical Research*, v. 108, no. B7, 2346, doi:10.1029/2002JB002080.
- Craddock, W., Kirby, E., and Zhang, H., 2011, Late Miocene-Pliocene range growth in the interior of the northeastern Tibetan Plateau: *Lithosphere*, v. 3, p. 420–438, doi:10.1130/L159.1.
- Dai, S., Fang, X., Dupont-Nivet, G., Song, C., Gao, J., Krijgsman, W., Langereis, C., and Zhang, W., 2006, Magnetostratigraphy of Cenozoic sediments from the Xining Basin: Tectonic implications for the northeastern Tibetan Plateau: *Journal of Geophysical Research*, v. 111, B11102, doi:10.1029/2005JB004187.
- Dang, J., 2011, Geochemical characteristics and tectonic implications of Jinfosi granite in north Qilian: *Gansu Geology*, v. 20, p. 40–44.
- Dewey, J.F., Shackelton, R.M., Chang, C., and Sun, Y., 1988, The tectonic evolution of the Tibetan Plateau: *Philosophical Transactions of the Royal Society of London*, v. A327, p. 379–413.
- Dong, Z., Wang, H., Guo, C., Xu, X., Chen, J., and He, S., 2009, Geochemical characteristics of Ordovician Honghuapu intrusions in the west segment of North Qinling Mountains and their geological significance: *Acta Petrologica et Mineralogica*, v. 28, p. 109–117.
- Dupont-Nivet, G., Horton, B.K., Butler, R.F., Wang, J., Zhou, J., and Waanders, G.L., 2004, Paleogene clockwise tectonic rotation of the Xining-Lanzhou region, northeastern Tibetan Plateau: *Journal of Geophysical Research*, v. 109, B04401, doi:10.1029/2003JB002620.
- Duvall, A.R., Clark, M.K., van der Pluijm, B.A., and Li, C., 2011, Direct dating of Eocene reverse faulting in northeastern Tibet using Ar-dating of fault clays and low-temperature thermochronometry: *Earth and Planetary Science Letters*, v. 304, p. 520–526, doi:10.1016/j.epsl.2011.02.028.
- England, P., and Houseman, G., 1986, Finite strain calculations of continental deformation: 2. Comparison with the India-Asia collision zone: *Journal of Geophysical Research*, v. 91, p. 3664–3676, doi:10.1029/JB091iB03p3664.
- England, P., and Houseman, G., 1989, Extension during continental convergence, with application to the Tibetan Plateau: *Journal of Geophysical Research*, v. 94, p. 17,561–17,569, doi:10.1029/JB094iB12p17561.
- Fang, X., Yan, M., Van der Voo, R., Rea, D.K., Song, C., Parés, J.M., Gao, J., Nie, J., and Dai, S., 2005, Late Cenozoic deformation and uplift of the NE Tibetan Plateau: Evidence from high-resolution magnetostratigraphy of the Guide Basin, Qinghai Province, China: *Geological Society of America Bulletin*, v. 117, p. 1208–1225, doi:10.1130/B25727.1.
- Gao, R., Cheng, X., and Wu, G., 1999, Lithospheric structure and geodynamic model of the Golmud-Ejin transect in northern Tibet, in Macfarlane, A., Sorkhabi, R.B., and Quade, J., eds., *Himalaya and Tibet: Mountain Roots to Mountain Tops*: Geological Society of America Special Paper 328, p. 9–17.
- Gao, R., Huang, D., Lu, D., Qian, G., Li, Y., Kuang, C., Li, Q., Li, P., Feng, R., and Guan, Y., 2000, Deep seismic reflection profile across the juncture zone between the Tarim Basin and the western Kunlun Range: *Chinese Science Bulletin*, v. 45, p. 2281–2286, doi:10.1007/BF02886369.
- Gao, R., Li, P., Li, Q., Guan, Y., Shi, D., Kong, X., and Liu, H., 2001, Deep process of the collision and deformation on the northern margin of the Tibetan Plateau: Revelation from investigation of the deep seismic profiles: *Science in China*, v. 44, p. 71–78, doi:10.1007/BF02911973.
- Garzone, C.N., Ikari, M.J., and Basu, A.R., 2005, Source of Oligocene to Pliocene sedimentary rocks in the Linxia Basin in northeastern Tibet from Nd isotopes: Implications for tectonic forcing of climate: *Geological Society of America Bulletin*, v. 117, p. 1156–1166, doi:10.1130/B25743.1.
- Gaudemer, Y., Tapponnier, P., Meyer, B., Peltzer, G., Shunmin, G., Zhitai, C., Huagang, D., and Cifuentes, I., 1995, Par-

- titoning of crustal slip between linked, active faults in the eastern Qilian Shan, and evidence for a major seismic gap, the 'Tianzhu gap', on the western Haiyuan fault, Gansu (China): *Geophysical Journal International*, v. 120, p. 599–645, doi:10.1111/j.1365-246X.1995.tb01842.x.
- Gehrels, G.E., Yin, A., and Wang, X.-F., 2003a, Detrital-zircon geochronology of the northeastern Tibetan Plateau: *Geological Society of America Bulletin*, v. 115, p. 881–896, doi:10.1130/0016-7606(2003)115<0881:DGOTNT>2.0.CO;2.
- Gehrels, G.E., Yin, A., and Wang, X.-F., 2003b, Magmatic history of the northeastern Tibetan Plateau: *Journal of Geophysical Research*, v. 108, 2423, doi:10.1029/2002JB001876.
- Grujic, D., Casey, M., Davidson, C., Hollister, L.S., Kundig, R., Pavlis, T., and Schmid, S., 1996, Ductile extrusion of the Higher Himalayan Crystalline in Bhutan: Evidence from quartz microfibrils: *Tectonophysics*, v. 260, p. 21–43, doi:10.1016/0040-1951(96)00074-1.
- Guo, J., Hao, F., and Li, H., 1999, Jinningian collisional granite belt in the eastern sector of the central Qilian massif and its implication: *Acta Geoscientia Sinica*, v. 20, p. 10–15.
- Guo, X., Yan, Z., Wang, Z., Wang, T., Hou, K., Fu, C., and Li, J., 2012, Middle Triassic arc magmatism along the northeastern margin of the Tibet: U-Pb and Lu-Hf zircon characterization of the Gangcha complex in the West Qinling terrane, central China: *Journal of the Geological Society of London*, v. 169, p. 327–336, doi:10.1144/0016-76492011-083.
- Harrison, T.M., Copeland, P., Kidd, W.S.F., and Yin, A., 1992, Raising Tibet: *Science*, v. 255, p. 1663–1670, doi:10.1126/science.255.5052.1663.
- He, S., Kapp, P., DeCelles, P.G., Gehrels, G.E., and Heizler, M., 2007a, Cretaceous–Tertiary geology of the Gangdese Arc in the Linzhou area, southern Tibet: *Tectonophysics*, v. 433, p. 15–37, doi:10.1016/j.tecto.2007.01.005.
- He, S., Wang, H., Xu, X., Zhang, H., and Ren, G., 2007b, A LA-ICP-MS U-Pb chronological study of zircons from Hongtubu basic volcanic rocks and its geological significance in the east segment of North Qilian orogenic belt: *Advances in Earth Science*, v. 22, p. 143–151.
- Hetzl, R., Tao, M., Stokes, S., Niedermann, S., Ivy-Ochs, S., Gao, B., Strecker, M.R., and Kubik, P.W., 2004, Late Pleistocene/Holocene slip rate of the Zhangye thrust (Qilian Shan, China) and implications for the active growth of the northeastern Tibetan Plateau: *Tectonics*, v. 23, TC6006, doi:10.1029/2004TC001653.
- Horton, B.K., Dupont-Nivet, G., Zhou, J., Waanders, G.L., Butler, R.F., and Wang, J., 2004, Mesozoic–Cenozoic evolution of the Xining–Minhe and Dangchang Basins, northeastern Tibetan Plateau: Magnetostratigraphic and biostratigraphic results: *Journal of Geophysical Research*, v. 109, B04402, doi:10.1029/2003JB002913.
- Hubbard, J., and Shaw, J.H., 2009, Uplift of the Longmen Shan and Tibetan Plateau, and the 2008 Wenchuan (M57.9) earthquake: *Nature*, v. 458, p. 194–197, doi:10.1038/nature07837.
- Huo, Y. L., and Tan, S.D., 1995, Exploration Case History and Petroleum Geology in Jiuquan Continental Basin: Beijing, Petroleum Industry Press, 211 p.
- Jin, W., Zhang, Q., He, D., and Jia, X., 2005, Shrimp dating of adakites in western Qinling and their implications: *Acta Petrolei Sinica*, v. 21, p. 959–966.
- Jin, Z., Cunningham, D., and Hongyi, C., 2010, Sedimentary characteristics of Cenozoic strata in central-southern Ningxia, NW China: Implications for the evolution of the NE Qinghai–Tibetan Plateau: *Journal of Asian Earth Sciences*, v. 39, p. 740–759, doi:10.1016/j.jseaes.2010.05.008.
- Jolivet, M., Brunel, M., Seward, D., Xu, Z., Yang, J., Roger, F., Tapponnier, P., Malavielle, J., Arnaud, N., and Wu, C., 2001, Mesozoic and Cenozoic tectonics of the northern edge of the Tibetan Plateau: Fission-track constraints: *Tectonophysics*, v. 343, p. 111–134, doi:10.1016/S0040-1951(01)00196-2.
- Jolivet, R., Lasserre, C., Doin, M.P., Guillaso, S., Peltzer, G., Dailu, R., Sun, J., Shen, Z.K., and Xu, X., 2012, Shallow creep on the Haiyuan fault (Gansu, China) revealed by SAR interferometry: *Journal of Geophysical Research*, v. 117, B06401, doi:10.1029/2011JB008732.
- Judge, P.A., and Allmendinger, R.W., 2011, Assessing uncertainties in balanced cross sections: *Journal of Structural Geology*, v. 33, p. 458–467, doi:10.1016/j.jsg.2011.01.006.
- Kapp, P., Yin, A., Manning, C.E., Murphy, M., Harrison, T.M., Spurlin, M., Lin, D., Xi-Guang, D., and Cun-Ming, W., 2000, Blueschist-bearing metamorphic core complexes in the Qiangtang block reveal deep crustal structure of northern Tibet: *Geology*, v. 28, p. 19–22, doi:10.1130/0091-7613(2000)28<19:BMCCIT>2.0.CO;2.
- Karplus, M.S., Zhao, W., Klempner, S.L., Wu, Z., Mechie, J., Shi, D., Brown, L.D., and Chen, C., 2011, Injection of Tibetan crust beneath the south Qaidam Basin: Evidence from INDEPTH IV wide-angle seismic data: *Journal of Geophysical Research*, v. 116, B07301, doi:10.1029/2010JB007911.
- Kind, R., Yuan, X., Saul, J., Nelson, D., Sobolev, S.V., Mechie, J., Zhao, W., Kosarev, G., Ni, J., Achauer, U., and Jiang, M., 2002, Seismic images of crust and upper mantle beneath Tibet: Evidence for Eurasian plate subduction: *Science*, v. 298, p. 1219–1221, doi:10.1126/science.1078115.
- Kumar, P., Yuan, X., Kind, R., and Ni, J., 2006, Imaging the colliding Indian and Asian lithospheric plates beneath Tibet: *Journal of Geophysical Research*, v. 111, B06308, doi:10.1029/2005JB003930.
- Lasserre, C., Morel, P.H., Gaudemer, Y., Tapponnier, P., Ryerson, F.J., King, G.C.P., Métiévier, F., Kasser, M., Kashgarian, M., Baihi, L., Taiya, L., and Daoyang, Y., 1999, Postglacial left slip rate and past occurrence of M ≥ 8 earthquakes on the western Haiyuan fault, Gansu, China: *Journal of Geophysical Research*, v. 104, p. 17633–17651, doi:10.1029/1998JB900082.
- Lasserre, C., Gaudemer, Y., Tapponnier, P., Mériaux, A.S., Van der Woerd, J., Daoyang, Y., Ryerson, F.J., Finkel, R.C., and Caffee, M.W., 2002, Fast late Pleistocene slip rate on the Leng Long Ling segment of the Haiyuan fault, Qinghai, China: *Journal of Geophysical Research*, v. 107, 2276, doi:10.1029/2000JB000060.
- Lease, R.O., Burbank, D.W., Gehrels, G.E., Wang, Z., and Yuan, D., 2007, Signatures of mountain building: Detrital zircon U/Pb ages from northeastern Tibet: *Geology*, v. 35, p. 239–242, doi:10.1130/G23057A.1.
- Lease, R.O., Burbank, D.W., Clark, M.K., Farley, K.A., Zheng, D., and Zhang, H., 2011, Middle Miocene reorganization of deformation along the northeastern Tibetan Plateau: *Geology*, v. 39, p. 359–362, doi:10.1130/G31356.1.
- Lease, R.O., Burbank, D.W., Hough, B., Wang, Z., and Yuan, D., 2012a, Pulsed Miocene range growth in northeastern Tibet: Insights from Xunhua Basin magnetostratigraphy and provenance: *Geological Society of America Bulletin*, v. 124, p. 657–677, doi:10.1130/B30524.1.
- Lease, R.O., Burbank, D.W., Zhang, H., Liu, J., and Yuan, D., 2012b, Cenozoic shortening budget for the northeastern edge of the Tibetan Plateau: Is lower crustal flow necessary? *Tectonics*, v. 31, TC3011, doi:10.1029/2011TC003066.
- Li, J., Wang, X., and Niu, F., 2011, Seismic anisotropy and implications for mantle deformation beneath the NE margin of the Tibet Plateau and Ordos Plateau: *Physics of the Earth and Planetary Interiors*, v. 189, p. 157–170, doi:10.1016/j.pepi.2011.08.009.
- Li, Y.J., Gao, Z.H., Li, Y., Li, Z.C., and Liu, Z.B., 2003, The geochemical features of the Wenquan magma-mingling granite in Western Qinling: *Geology Geochemistry*, v. 31, p. 43–49 (in Chinese).
- Li, Y., Wu, Q., Zhang, F., Feng, Q., and Zhang, R., 2011, Seismic anisotropy of the northeastern Tibetan Plateau from shear wave splitting analysis: *Earth and Planetary Science Letters*, v. 304, p. 147–157, doi:10.1016/j.epsl.2011.01.026.
- Liang, X., Sandvol, E., Chen, Y.J., Hearn, T., Ni, J., Klempner, S., Shen, Y., and Tilmann, F., 2012, A complex Tibetan upper mantle: A fragmented Indian slab and no south-verging subduction of Eurasian lithosphere: *Earth and Planetary Science Letters*, v. 333–334, p. 101–111, doi:10.1016/j.epsl.2012.03.036.
- Lin, X., Chen, H., Wyrwoll, K.-H., Batt, G.E., Liao, L., and Xiao, J., 2011, The uplift history of the Haiyuan–Liupan Shan region northeast of the present Tibetan Plateau: Integrated constraints from stratigraphy and thermochronology: *The Journal of Geology*, v. 119, p. 372–393, doi:10.1086/660190.
- Liu, D., Yan, M., Fang, X., Li, H., Song, C., and Dai, S., 2011, Magnetostratigraphy of sediments from the Yumu Shan, Hexi Corridor, and its implications regarding the late Cenozoic uplift of the NE Tibetan Plateau: *Quaternary International*, v. 236, p. 13–20, doi:10.1016/j.quaint.2010.12.007.
- Liu, M.J., Mooney, W.D., Li, S.L., Okaya, N., and Detweiler, S., 2006, Crustal structure of the northeastern margin of the Tibetan Plateau from the Songpan–Ganzi terrane to the Ordos basin: *Tectonophysics*, v. 420, p. 253–266, doi:10.1016/j.tecto.2006.01.025.
- Liu, Y.-J., Neubauer, F., Genser, J., Takasu, A., Ge, X.-H., and Handler, R., 2006, <sup>40</sup>Ar/<sup>39</sup>Ar ages of blueschist facies pelitic schists from Qingshuigou in the northern Qilian Mountains, western China: *The Island Arc*, v. 15, p. 187–198, doi:10.1111/j.1440-1738.2006.00508.x.
- Lu, H., Wang, E., Shi, X., and Meng, K., 2012, Cenozoic tectonic evolution of the Elashan range and its surroundings, northern Tibetan Plateau, as constrained by paleomagnetism and apatite fission track analyses: *Tectonophysics*, v. 580, p. 150–161, doi:10.1016/j.tecto.2012.09.013.
- Luo, B., Zhang, H., and Xiao, Z., 2012, Petrogenesis and tectonic implications of the early Indosinian Meiwu pluton in West Qinling, central China: *Earth Science Frontiers*, v. 19, p. 199–213.
- Meyer, B., Tapponnier, P., Bourjot, L., Métiévier, F., Gaudemer, Y., Peltzer, G., Shunmin, G., and Zhitai, C., 1998, Crustal thickening in Gansu–Qinghai, lithospheric mantle subduction, and oblique, strike-slip controlled growth of the Tibet Plateau: *Geophysical Journal International*, v. 135, p. 1–47, doi:10.1046/j.1365-246X.1998.00567.x.
- Molnar, P., England, P., and Martinod, J., 1993, Mantle dynamics, the uplift of the Tibetan Plateau, and the Indian monsoon: *Reviews of Geophysics*, v. 31, p. 357–396, doi:10.1029/93RG02030.
- Murphy, M.A., Yin, A., Harrison, T.M., Durr, S.B., Chen, Z., Ryerson, F.J., Kidd, W.S.F., Wang, X., and Zhou, X., 1997, Did the Indo-Asian collision alone create the Tibetan Plateau? *Geology*, v. 25, p. 719–722, doi:10.1130/0091-7613(1997)025<0719:DTIACA>2.3.CO;2.
- Nelson, K.D., and 27 others, 1996, Partially molten middle crust beneath southern Tibet: Synthesis of project INDEPTH results: *Science*, v. 274, p. 1684–1688, doi:10.1126/science.274.5293.1684.
- Pan, G., Ding, J., Yao, D., and Wang, L., 2004, Geological map of Qinghai–Xiang (Tibet) plateau and adjacent areas (1:1,500,000): Chengdu Institute of Geology and Mineral Resources, China Geological Survey, Chengdu Cartographic Publishing House, Chengdu, China.
- Pei, X., Li, Y., Lu, S., Chen, Z., Ding, S., Hu, B., Li, Z., and Liu, H., 2005, Zircon U–Pb ages of the Guanzhizhen intermediate-basic igneous complex in Tianshui area, West Qinling, and their geological significance: *Geological Bulletin of China*, v. 24, p. 23–29.
- Pei, X., Ding, S., Zhang, G., Liu, H., Li, Z., Li, G., Liu, Z., and Meng, Y., 2007a, Geochemical characteristics and LA-ICP-MS zircon U–Pb dating of Baihua igneous complexes in the Tianshui area, West Qinling: *Science in China, ser. D, Earth Sciences*, v. 37, p. 224–234.
- Pei, X., Sun, R., Ding, S., Liu, H., Li, Z., Liu, Z., and Meng, Y., 2007b, LA-ICP-MS zircon U–Pb dating of the Yanjiadian diorite in the eastern Qilian Mountains and its geological significance: *Geology in China*, v. 34, p. 8–16.
- Pei, X., Li, Z., Liu, H., Li, G., Ding, S., Li, Y., Hu, B., and Guo, J., 2007c, Geochemical characteristics and zircon U–Pb isotopic ages of island-arc basic igneous complexes from the Tianshui area in West Qinling: *Frontiers of Earth Science in China*, v. 1, p. 49–59, doi:10.1007/s11707-007-0008-3.
- Pei, X., Ding, S., Li, Z., Liu, Z., Li, R., Feng, J., Sun, Y., Zhang, Y., Liu, Z., Zhang, X., Chen, G., and Chen, Y., 2009, Early Paleozoic Tianshui–Wushan tectonic zone of the northern margin of West Qinling and its tectonic evolution: *Acta Geologica Sinica*, v. 83, p. 1547–1564.
- Quan, S., Jia, Q., Guo, Z., and Wang, W., 2006, Basic characteristics of granitoids related to tungsten mineralization in the Qilian mountain: *Mineralium Deposita*, v. 25, p. 143–146.
- Royden, L.H., Burchfiel, B.C., King, R.W., Wang, E., Chen, Z., Shen, F., and Liu, Y., 1997, Surface deformation and lower crustal flow in eastern Tibet: *Science*, v. 276, p. 788–790, doi:10.1126/science.276.5313.788.
- Royden, L.H., Burchfiel, B.C., and van der Hilst, R.D., 2008, The geological evolution of the Tibetan Plateau: *Science*, v. 321, p. 1054–1058, doi:10.1126/science.1155371.
- Seong, Y.B., Kang, H.-C., Ree, J.-H., Choi, J.-H., Lai, Z., Long, H., and Yoon, H.O., 2011, Geomorphic constraints on active mountain growth by the lateral propagation of

- fault-related folding: A case study on Yumu Shan, NE Tibet: *Journal of Asian Earth Sciences*, v. 41, p. 184–194, doi:10.1016/j.jseas.2011.01.015.
- Shi, D., Zhao, W., Brown, L., Nelson, D., Zhao, X., Kind, R., Ni, J., Xiong, J., Mechie, J., Guo, J., Klempner, S., and Hearn, T., 2004, Detection of southward intracontinental subduction of Tibetan lithosphere along the Bangong-Nujiang suture by Pto-S converted waves: *Geology*, v. 32, p. 209–212, doi:10.1130/G19814.1.
- Smith, A.D., 2006, The geochemistry and age of ophiolitic strata of the Xinglongshan Group: Implications for the amalgamation of the Central Qilian belt: *Journal of Asian Earth Sciences*, v. 28, p. 133–142, doi:10.1016/j.jseas.2005.09.014.
- Sobel, E.R., and Arnaud, N., 1999, A possible middle Paleozoic suture in the Altyn Tagh, NW China: *Tectonics*, v. 18, p. 64–74, doi:10.1029/1998TC900023.
- Song, S., Su, L., Li, X.-H., Niu, Y., and Zhang, L., 2012, Grenville-age orogenesis in the Qaidam-Qilian block: The link between South China and Tarim: *Precambrian Research*, v. 220–221, p. 9–22, doi:10.1016/j.precamres.2012.07.007.
- Song, S., Niu, Y., Su, L., and Xia, X., 2013, Tectonics of the North Qilian Orogen, NW China: *Gondwana Research*, v. 23, p. 1378–1401.
- Su, J., Zhang, X., Hu, N., Fu, G., and Zhang, H., 2004, Geochemical characteristics and genesis of adakite-like granites at Yema Nanshan in the western segment of the Central Qilian Mountains: *Chinese Geology*, v. 31, p. 365–371.
- Tapponnier, P., Meyer, B., Avouac, J.P., Peltzer, G., Gaudemer, Y., Guo, S., Xiang, H., Yin, K., Chen, Z., Cai, S., and Dai, H., 1990, Active thrusting and folding in the Qilian Shan, and decoupling between upper crust and mantle in northeastern Tibet: *Earth and Planetary Science Letters*, v. 97, p. 382–403, doi:10.1016/0012-821X(90)90053-Z.
- Tapponnier, P., Zhiqin, X., Roger, F., Meyer, B., Arnaud, N., Wittlinger, G., and Jingsui, Y., 2001, Oblique stepwise rise and growth of the Tibet Plateau: *Science*, v. 294, p. 1671–1677, doi:10.1126/science.105978.
- Taylor, M., and Yin, A., 2009, Active structures of the Himalayan-Tibetan orogen and their relationships to earthquake distribution, contemporary strain field, and Cenozoic volcanism: *Geosphere*, v. 5, no. 3, p. 199–214, doi:10.1130/GES00217.1.
- Tseng, C.Y., Yang, H.Y., Yusheng, W., Dunyi, L., Wen, D.J., Lin, T.C., and Tung, K.A., 2006, Finding of Neoproterozoic (775 Ma) magmatism recorded in metamorphic complexes from the North Qilian orogen: Evidence from SHRIMP zircon U-Pb dating: *Chinese Science Bulletin*, v. 51, p. 963–970, doi:10.1007/s11434-006-0963-1.
- Tseng, C.Y., Yang, H.J., Yang, H.Y., Liu, D., Tsai, C.L., Wu, H., and Zuo, G., 2007, The Dongcaohé ophiolite from the North Qilian Mountains: A fossil oceanic crust of the paleo-Qilian ocean: *Chinese Science Bulletin*, v. 52, p. 2390–2401, doi:10.1007/s11434-007-0300-3.
- Tseng, C.Y., Yang, H.J., Yang, H.Y., Liu, D., Wu, C., Cheng, C.K., Chen, C.H., and Ker, C.M., 2009a, Continuity of the North Qilian and North Qinling orogenic belts, central orogenic system of China: Evidence from newly discovered Paleozoic adakitic rocks: *Gondwana Research*, v. 16, p. 285–293, doi:10.1016/j.gr.2009.04.003.
- Tseng, C.Y., Zuo, G.C., Yang, H.J., Yang, H.Y., Tung, K.A., Liu, D.Y., and Wu, H.Q., 2009b, Occurrence of Alaskan-type mafic-ultramafic intrusions in the North Qilian Mountains, northwest China: Evidence of Cambrian arc magmatism on the Qilian block: *The Island Arc*, v. 18, p. 526–549, doi:10.1111/j.1440-1738.2009.00675.x.
- Tung, K., Yang, H.J., Yang, H.Y., Liu, D., Zhang, J., Wan, Y., and Tseng, C.Y., 2007a, SHRIMP U-Pb geochronology of the zircons from the Precambrian basement of the Qilian block and its geological significances: *Chinese Science Bulletin*, v. 52, p. 2687–2701, doi:10.1007/s11434-007-0356-0.
- Tung, K., Yang, H., Liu, D., Zhang, J., Tseng, C., and Wan, Y., 2007b, SHRIMP U-Pb geochronology of the detrital zircons from the Longshoushan Group and its tectonic significance: *Chinese Science Bulletin*, v. 52, p. 1414–1425, doi:10.1007/s11434-007-0189-x.
- Tung, K.A., Yang, H.Y., Liu, D.Y., Zhang, J.X., Yang, H.J., Shau, Y.H., and Tseng, C.Y., 2012, The amphibolite-facies metamorphosed mafic rocks from the Maxianshan area, Qilian block, NW China: A record of early Neoproterozoic arc magmatism: *Journal of Asian Earth Sciences*, v. 46, p. 177–189, doi:10.1016/j.jseas.2011.12.006.
- Van der Woerd, J., Xiwei, X., Haibing, L., Tapponnier, P., Meyer, B., Ryerson, F.J., Meriaux, A.S., and Zhiqin, X., 2001, Rapid active thrusting along the northwestern range front of the Tanghe Nan Shan (western Gansu, China): *Journal of Geophysical Research*, v. 106, p. 30,475–30,504, doi:10.1029/2001JB000583.
- Vincent, S.J., and Allen, M.B., 1999, Evolution of the Minle and Chaoshui Basins, China: Implications for Mesozoic strike-slip basin formation in Central Asia: *Geological Society of America Bulletin*, v. 111, p. 725–742, doi:10.1130/0016-7606(1999)111<0725:EOTMAC>2.3.CO;2.
- Wan, Y., Xu, Z., Yang, J., and Zhang, J., 2001, Ages and compositions of the Precambrian high-grade basement of the Qilian terrane and its adjacent areas: *Acta Geologica Sinica—English Edition*, v. 75, p. 375–384.
- Wan, Y., Xu, Z., Yang, J., and Zhang, J., 2003, The Precambrian high-grade basement of the Qilian terrane and neighboring areas: Its ages and compositions: *Acta Geologica Sinica*, v. 24, p. 319–324.
- Wang, C.S., Gao, R., Yin, A., Wang, H.Y., Zhang, Y.X., Guo, T., Li, Q., and Li, Y.L., 2011, A mid-crustal strain-transfer model for continental deformation: A new perspective from high-resolution deep seismic-reflection profiling across NE Tibet: *Earth and Planetary Science Letters*, v. 306, p. 279–288, doi:10.1016/j.epsl.2011.04.010.
- Wang, H., He, S., Chen, J., Xu, X., Song, Y., and Diwu, C., 2007, LA-ICPMS dating of zircon U-Pb and its tectonic significance of Maxianshan granitoid intrusive complex, Gansu Province: *Acta Geologica Sinica*, v. 81, p. 72–78.
- Wang, J.H., Yin, A., Harrison, T.M., Grove, M., Zhang, Y.Q., and Xie, G.H., 2001, A tectonic model for Cenozoic igneous activities in the eastern Indo-Asian collision zone: *Earth and Planetary Science Letters*, v. 188, p. 123–133, doi:10.1016/S0012-821X(01)00315-6.
- Wang, W.T., Zhang, P.Z., Kirby, E., Wang, L.H., Zhang, G.L., Zheng, D.W., and Chai, C.Z., 2011, A revised chronology for Tertiary sedimentation in the Sikouzi Basin: Implications for the tectonic evolution of the northeastern corner of the Tibetan Plateau: *Tectonophysics*, v. 505, p. 100–114, doi:10.1016/j.tecto.2011.04.006.
- Wang, X., Zattin, M., Li, J., Song, C., Peng, T., Liu, S., and Liu, B., 2011, Eocene to Pliocene exhumation history of the Tienshui-Huicheng region determined by apatite fission track thermochronology: Implications for evolution of the northeastern Tibetan Plateau margin: *Journal of Asian Earth Sciences*, v. 42, p. 97–110, doi:10.1016/j.jseas.2011.04.012.
- Wang, Z., Zhang, P., Garzone, C.N., Lease, R.O., Zhang, G., Zheng, D., Hough, B., Yuan, D., Li, C., Liu, J., and Wu, Q., 2012, Magnetostratigraphy and depositional history of the Miocene Wushan basin on the NE Tibetan Plateau, China: Implications for middle Miocene tectonics of the West Qinling fault zone: *Journal of Asian Earth Sciences*, v. 44, p. 189–202, doi:10.1016/j.jseas.2011.06.009.
- Webb, A.A.G., Yin, A., Harrison, T.M., Célérier, J., Gehrels, G.E., Grove, M., Manning, M.E., and Burgess, W.P., 2011, Cenozoic tectonic history of the Himalach Himalaya (northwestern India) and its constraints on the formation mechanism of the Himalayan orogen: *Geosphere*, v. 7, p. 1013–1061, doi:10.1130/GES00627.1.
- Wu, C.L., Yang, J.S., Yang, H.Y., Wooden, J., Shi, R.D., Chen, S.Y., and Zheng, Q.G., 2004, Dating of two types of granite from north Qilian, China: *Acta Petrologica Sinica*, v. 20, p. 425–432.
- Wu, C., Yao, S., Zeng, L., Yang, J., Wooden, J., Chen, S., and Mazadab, F., 2006, Double subduction of the early Paleozoic North Qilian oceanic plate: Evidence from granites in the central segment of North Qilian, NW China: *Geology in China*, v. 33, p. 1197–1208.
- Wu, C.L., Xu, X.Y., Gao, Q.M., Li, X.M., Lei, M., Gao, Y.H., Frost, B.R., and Wooden, J., 2010, Early Palaeozoic granitoid magmatism and tectonic evolution in North Qilian, NW China: *Acta Petrologica Sinica*, v. 26, p. 1027–1044 (in Chinese with English abstract).
- Xia, X., and Song, S., 2010, Forming age and tectono-petrogenesis of the Jiugequan ophiolite in the North Qilian Mountain, NW China: *Chinese Science Bulletin*, v. 55, p. 1899–1907, doi:10.1007/s11434-010-3207-3.
- Xia, X., Song, S., and Niu, Y., 2012, Tholeiite-boninite terrane in the North Qilian suture zone: Implications for subduction initiation and back-arc basin development: *Chemical Geology*, v. 328, p. 259–277, doi:10.1016/j.chemgeo.2011.12.001.
- Xiao, G., Guo, Z., Dupont-Nivet, G., Lu, H., Wu, N., Ge, J., Hao, Q., Peng, S., Li, F., Abels, H.A., and Zhang, K., 2012, Evidence for northeastern Tibetan Plateau uplift between 25 and 200 Ma in the sedimentary archive of the Xining Basin, northwestern China: *Earth and Planetary Science Letters*, v. 317–318, p. 185–195, doi:10.1016/j.epsl.2011.11.008.
- Xiao, W., Windley, B.F., Yong, Y., Yan, Z., Yuan, C., Liu, C., and Li, J., 2009, Early Paleozoic to Devonian multiple-accretionary model for the Qilian Shan, NW China: *Journal of Asian Earth Sciences*, v. 35, p. 323–333, doi:10.1016/j.jseas.2008.10.001.
- Xiong, Z., Zhang, H., and Zhang, J., 2012, Petrogenesis and tectonic implications of the Maozangsi and Huangyanghe granitic intrusions in Lenglongling area, the eastern part of North Qilian Mountain, NW China: *Earth Science Frontiers*, v. 19, p. 214–227.
- Xu, X., He, S., Wang, H., Zhang, E., Chen, J., and Sun, J., 2008a, Tectonic framework of the North Qilian mountain and North Qilian Mountain conjunction area in early Paleozoic: A study of the evidence from strata and tectono-magmatic events: *Northeastern Geology*, v. 41, p. 1–21.
- Xu, Y.-J., Du, Y.-S., Cawood, P.A., Guo, H., Huang, H., and An, Z.-H., 2010a, Detrital zircon record of continental collision: Assembly of the Qilian orogen, China: *Sedimentary Geology*, v. 230, p. 35–45, doi:10.1016/j.sedgeo.2010.06.020.
- Xu, Y.-J., Du, Y., Cawood, P.A., and Yang, J., 2010b, Provenance record of a foreland basin: Detrital zircon U-Pb ages from Devonian strata in the North Qilian orogenic belt, China: *Tectonophysics*, v. 495, p. 337–347, doi:10.1016/j.tecto.2010.10.001.
- Xue, N., Wang, J., Tan, S.-x., Lin, H., Li, W.-f., Ren, J.-q., and Liu, S.-j., 2009, Geological significance of granite of Jinningian age in Yenuigou-Toule region on the northern margin of Central Qilian block: *Journal of Qinghai University*, v. 27, p. 23–28.
- Yan, Z., Xiao, W.J., Windley, B.F., Wang, Z.Q., and Li, J.L., 2010, Silurian clastic sediments in the North Qilian Shan, NW China: Chemical and isotopic constraints on their forearc provenance with implications for the Paleozoic evolution of the Tibetan Plateau: *Sedimentary Geology*, v. 231, p. 98–114, doi:10.1016/j.sedgeo.2010.09.001.
- Yang, J.H., Du, Y.S., Cawood, P.A., and Xu, Y.J., 2009, Silurian collisional suturing onto the southern margin of the North China craton: Detrital zircon geochronology constraints from the Qilian orogen: *Sedimentary Geology*, v. 220, p. 95–104, doi:10.1016/j.sedgeo.2009.07.001.
- Yang, J., Du, Y., Cawood, P.A., and Xu, Y., 2012, From subduction to collision in the northern Tibetan Plateau: Evidence from the Early Silurian clastic rocks, northwestern China: *The Journal of Geology*, v. 120, p. 49–67, doi:10.1086/662717.
- Yang, Y., Ritzwoller, M.H., Zheng, Y., Shen, W., Levshin, A.L., and Xie, Z., 2012, A synoptic view of the distribution and connectivity of the mid-crustal low velocity zone beneath Tibet: *Journal of Geophysical Research*, v. 117, B04303, doi:10.1029/2011JB008810.
- Yin, A., 2010, A special issue on the great 12 May 2008 Wenchuan earthquake (Mw7.9): Observations and unanswered questions: *Tectonophysics*, v. 491, p. 1–9, doi:10.1016/j.tecto.2010.05.019.
- Yin, A., and Harrison, T.M., 2000, Geologic evolution of the Himalayan-Tibetan orogen: *Annual Review of Earth and Planetary Sciences*, v. 28, p. 211–280, doi:10.1146/annurev.earth.28.1.211.
- Yin, A., Rumelhart, P.E., Butler, R., Cowgill, E., Harrison, T.M., Foster, D.A., Ingersoll, R.V., Zhang, Q., Zhou, X.Q., Wang, X.F., Hanson, A., and Raza, A., 2002, Tectonic history of the Altyn Tagh fault system in northern Tibet inferred from Cenozoic sedimentation: *Geological Society of America Bulletin*, v. 114, no. 10, p. 1257–1295, doi:10.1130/0016-7606(2002)114<1257:THOTAT>2.0.CO;2.
- Yin, A., Manning, C.E., Lovera, O., Menold, C.A., Chen, X., and Gehrels, G.E., 2007a, Early Paleozoic tectonic and thermomechanical evolution of ultrahigh-pressure (UHP) metamorphic rocks in the northern Tibetan Plateau, northwest China: *International Geology Review*, v. 49, p. 681–716, doi:10.2747/0020-6814.49.8.681.

- Yin, A., Dang, Y.Q., Zhang, McRivette, M.W., Burgess, W.P., and Chen, X.H., 2007b, Cenozoic tectonic evolution of Qaidam Basin and its surrounding regions (Part 2): Wedge tectonics in southern Qaidam Basin and the Eastern Kunlun Range, in Sears, J.W., Harms, T.A., and Evenchick, C.A., eds., *Whence the Mountains? Inquiries into the Evolution of Orogenic Systems: A Volume in Honor of Raymond A. Price*: Geological Society of America Special Paper 433, p. 369–390.
- Yin, A., Dang, Y.-Q., Zhang, M., Chen, X.-H., and McRivette, M.W., 2008a, Cenozoic tectonic evolution of the Qaidam Basin and its surrounding regions (Part 3): Structural geology, sedimentation, and regional tectonic reconstruction: *Geological Society of America Bulletin*, v. 120, p. 847–876, doi:10.1130/B26232.1.
- Yin, A., Dang, Y.-Q., Wang, L.-C., Jiang, W.-M., Zhou, S.-P., Chen, X.-H., Gehrels, G.E., and McRivette, M.W., 2008b, Cenozoic tectonic evolution of Qaidam Basin and its surrounding regions (Part 1): The southern Qilian Shan–Nan Shan thrust belt and northern Qaidam Basin: *Geological Society of America Bulletin*, v. 120, p. 813–846, doi:10.1130/B26180.1.
- Yin, A., Dubey, C.S., Kelty, T.K., Webb, A.A.G., Harrison, T.M., Chou, C.Y., and C el erier, J., 2010, Geologic correlation of the Himalayan orogen and Indian craton (part 2): Structural geology, geochronology and tectonic evolution of the eastern Himalaya: *Geological Society of America Bulletin*, v. 122, no. 3/4, p. 360–395, doi:10.1130/B26461.1.
- Yong, Y., Xiao, W., Yuan, C., Yan, Z., and Li, J., 2008, Geochronology and geochemistry of Paleozoic granitic plutons from the eastern Central Qilian and their tectonic implications: *Acta Petrolei Sinica*, v. 24, p. 855–866.
- Yuan, D.Y., Champagnac, J.D., Ge, W.P., Molnar, P., Zhang, P.Z., Zheng, W.J., Zhang, H.P., and Liu, X.W., 2011, Late Quaternary right-lateral slip rates of faults adjacent to the lake Qinghai, northeastern margin of the Tibetan Plateau: *Geological Society of America Bulletin*, v. 123, p. 2016–2030, doi:10.1130/B30315.1.
- Yue, H., Chen, Y.J., Sandvol, E., Ni, J., Hearn, T., Zhou, S., Feng, Y., Ge, Z., Trujillo, A., Wang, Y., Jin, G., Jiang, M., Tang, Y., Liang, X., Wei, S., Wang, H., Fan, W., and Liu, Z., 2012, Lithospheric and upper mantle structure of the northeastern Tibetan Plateau: *Journal of Geophysical Research*, v. 117, B05307, doi:10.1029/2011JB008545.
- Zhang, H., Chen, Y., Xu, W., Liu, R., Yuan, H., and Liu, X., 2006, Granitoids around Gonghe basin in Qinghai province: Petrogenesis and tectonic implications: *Acta Petrolei Sinica*, v. 22, p. 2910–2922.
- Zhang, H.P., Craddock, W.H., Lease, R.O., Wang, W.t., Yuan, D.Y., Zhang, P.Z., Molnar, P., Zheng, D.W., and Zheng, W.J., 2012, Magnetostratigraphy of the Neogene Chaka basin and its implications for mountain building processes in the north-eastern Tibetan Plateau: *Basin Research*, v. 24, p. 31–50, doi:10.1111/j.1365-2117.2011.00512.x.
- Zhang, H.S., Teng, J., Tian, X., Zhang, Z., Gao, R., and Liu, J., 2012, Lithospheric thickness and upper-mantle deformation beneath the NE Tibetan Plateau inferred from S receiver functions and SKS splitting measurements: *Geophysical Journal International*, v. 191, p. 1285–1294.
- Zhang, J.X., Meng, F.C., and Wan, Y.S., 2007, A cold early Palaeozoic subduction zone in the North Qilian Mountains, NW China: Petrological and U-Pb geochronological constraints: *Journal of Metamorphic Geology*, v. 25, p. 285–304, doi:10.1111/j.1525-1314.2006.00689.x.
- Zhang, P., Burchfiel, B.C., Molnar, P., Zhang, W., Jiao, D., Deng, Q., Wang, Y., Royden, L., and Song, F., 1991, Amount and style of late Cenozoic deformation in the Liupan Shan area, Ningxia Autonomous Region, China: *Tectonics*, v. 10, p. 1111–1129, doi:10.1029/90TC02686.
- Zhang, Q., Sandvol, E., Ni, J., Yang, Y., and Chen, Y.J., 2011, Rayleigh wave tomography of the northeastern margin of the Tibetan Plateau: *Earth and Planetary Science Letters*, v. 304, p. 103–112, doi:10.1016/j.epsl.2011.01.021.
- Zhang, Z.J., Klempner, S., Bai, Z., Chen, Y., and Teng, J., 2011, Crustal structure of the Paleozoic Kunlun orogeny from an active-source seismic profile between Moba and Guide in East Tibet, China: *Gondwana Research*, v. 19, p. 994–1007, doi:10.1016/j.gr.2010.09.008.
- Zhang, Z.Q., McCaffrey, R., and Zhang, P., 2013, Relative motion across the eastern Tibetan Plateau: Contributions from faulting, internal strain and rotation rates: *Tectonophysics*, v. 22, p. 240–256.
- Zhao, W., and Morgan, W.J., 1987, Injection of Indian crust into Tibetan lower crust: A two-dimensional finite element model study: *Tectonics*, v. 6, p. 489–504, doi:10.1029/TC006i004p00489.
- Zhao, W., Kumar, P., Mechie, J., Kind, R., Meissner, R., Wu, Z., Shi, D., Su, H., Xue, G., Karplus, M., and Tilmann, F., 2011, Tibetan plate overriding the Asian plate in central and northern Tibet: *Nature Geoscience*, v. 4, p. 870–873, doi:10.1038/ngeo1309.
- Zheng, D., Clark, M.K., Zhang, P., Zheng, W., and Farley, K.A., 2010, Erosion, fault initiation and topographic growth of the North Qilian Shan (northern Tibetan Plateau): *Geosphere*, v. 6, p. 937–941, doi:10.1130/GES00523.1.
- Zheng, W.J., Zhang, P.Z., Yuan, D.Y., Zheng, D.W., Li, C., Zhang, P., Yin, J., Min, W., Heermance, R., and Chen, J., 2009, Deformation on the northern of the Tibetan Plateau from GPS measurement and geologic rates of the late Quaternary along the major fault: *Chinese Journal of Geophysics*, v. 52, p. 2491–2508.
- Zheng, W.J., Zhang, P.Z., He, W.G., Yuan, D.Y., Shao, Y.X., Zheng, D.W., Ge, W.P., and Min, W., 2013, Transformation of displacement between strike-slip and crustal shortening in the northern margin of the Tibetan Plateau: Evidence from decadal GPS measurements and late Quaternary slip rates on faults: *Tectonophysics*, v. 584, p. 267–280.
- Zhuang, G., Hourigan, J.K., Koch, P.L., Ritts, B.D., and Kent-Corson, M.L., 2011, Isotopic constraints on intensified aridity in Central Asia around 12–0 Ma: *Earth and Planetary Science Letters*, v. 312, p. 152–163, doi:10.1016/j.epsl.2011.10.005.

MANUSCRIPT RECEIVED 27 APRIL 2013  
 REVISED MANUSCRIPT RECEIVED 30 SEPTEMBER 2013  
 MANUSCRIPT ACCEPTED 16 OCTOBER 2013

Printed in the USA